



universität  
wien

## MASTERARBEIT / MASTER'S THESIS

Titel der Masterarbeit / Title of the Master's Thesis

„Limonoids as Liver X Receptor Modulators“

verfasst von / submitted by

Stefanie Stolzlechner, BSc.

angestrebter akademischer Grad / in partial fulfilment of the requirements for the degree of

Magistra pharmaciae (Mag.pharm.)

Wien, 2022 / Vienna 2022

Studienkennzahl lt. Studienblatt /  
degree programme code as it appears on  
the student record sheet:

UA 066 605

Studienrichtung lt. Studienblatt /  
degree programme as it appears on  
the student record sheet:

Masterstudium Pharmazie

Betreut von / Supervisor:

Univ.-Prof. Dr. Verena M. Dirsch



# Abstract

Atherosclerotic cardiovascular disease causes clinical endpoints such as myocardial infarction and stroke and represents the leading cause of death worldwide. The liver X receptor (LXR) implements a variety of regulatory roles in cholesterol metabolism, making it an excellent target in the treatment of atherosclerosis. Increased cholesterol efflux from lipid-laden macrophage foam cells provides protection against atherosclerotic plaque formation and disease progression.

The active compound used in this work named flindissone is a limonoid which was isolated from the leaves of *Trichilia prieuriana*. Luciferase reporter gene assays showed that flindissone is a novel LXR modulator, which can activate mainly LXR $\alpha$  and only slightly LXR $\beta$ . In the activation of LXR $\alpha$ , flindissone exhibits an EC<sub>50</sub> value of 1.4  $\mu$ M. A typical side effect of conventional LXR agonists is the development of hypertriglyceridemia with subsequent hepatic steatosis. This is primarily due to transcriptional induction of sterol regulatory element-binding protein 1c (SREBP1c), which is the dominant SREBP1 isoform in the liver. ATP binding cassette subfamily A member 1 (ABCA1) and ATP binding cassette subfamily G member 1 (ABCG1) are two major transporters involved in cholesterol efflux. The influence of flindissone on ABCA1, ABCG1 and SREBP1 expression was determined by Western blot and RT-qPCR experiments.

This work demonstrated, that flindissone is a novel LXR ligand that shows a clear tendency to induce the expression of ABCA1 and ABCG1 in THP-1 cells, but without causing a strong induction of SREBP1 expression in HepG2 cells.

# Zusammenfassung

Atherosklerotische Herz-Kreislauf-Erkrankungen verursachen klinische Endpunkte wie den Myokardinfarkt und Schlaganfall und stellen somit die häufigste Todesursache weltweit dar. Der Liver X Rezeptor (LXR) übernimmt eine Vielzahl an regulatorischen Aufgaben im Cholesterinmetabolismus und eignet sich deshalb als ein ausgezeichnetes Target in der Behandlung von Atherosklerose. Ein erhöhter Cholesterin-Efflux aus den lipidbeladenen Makrophagen-Schaumzellen bietet einen Schutz vor der Entwicklung von atherosklerotischen Plaques und der Progression der Erkrankung. Der in dieser Arbeit verwendete Wirkstoff namens Flindisson wurde aus den Blättern von *Trichilia prieuriana* isoliert und gehört zu der Gruppe der Limonoide. Luciferase Reporter Gen Assays zeigten, dass Flindisson einen neuartigen LXR Modulator darstellt, welcher vor allem LXR $\alpha$  und nur geringfügig LXR $\beta$  aktivieren kann. In der Aktivierung von LXR $\alpha$  weist Flindisson einen EC50 Wert von 1.4  $\mu$ M auf.

Eine typische Nebenwirkung herkömmlicher LXR Agonisten stellt die Entwicklung einer Hypertriglyceridämie mit einer nachfolgenden Lebersteatose dar. Dies ist vor allem auf die Transkriptionsinduktion von sterol regulatory element-binding protein 1c (SREBP1c) in der Leber zurückzuführen. ATP binding cassette subfamily A member 1 (ABCA1) und ATP binding cassette subfamily G member 1 (ABCG1) sind zwei Transporter, welche am Cholesterin-Efflux beteiligt sind. Der Einfluss von Flindisson auf die ABCA1, ABCG1 und SREBP1 Expression wurde durch Western Blot und RT-qPCR Experimente ermittelt.

In dieser Arbeit konnte gezeigt werden, dass Flindisson einen neuen LXR Liganden darstellt, welcher eine Tendenz aufweist, die Expression von ABCA1 und ABCG1 in THP-1 Zellen induzieren kann, ohne jedoch eine starke Erhöhung der SREBP1 Genexpression in HepG2 Zellen hervorzurufen.

## Table of content

<b>1</b>	<b><i>Introduction</i></b>	<b>1</b>
1.1	<b>Atherosclerosis</b>	<b>1</b>
1.1.1	Development of atherosclerosis	1
1.2	<b>Nuclear receptors</b>	<b>3</b>
1.2.1	Structure of nuclear receptors	4
1.2.2	Mechanism of action of nuclear receptors	5
1.3	<b>Liver X receptor</b>	<b>5</b>
1.4	<b>LXR target genes</b>	<b>7</b>
1.4.1	LXR activation in the intestine	7
1.4.2	LXR activation promotes cholesterol excretion in the liver	7
1.4.3	The role of LXR in reverse cholesterol transport	7
1.4.4	The importance of LXR in cholesterol uptake and biosynthesis in the liver	8
1.4.5	The problem of LXR activation in fatty acid metabolism	9
1.5	<b>Selective LXR modulators</b>	<b>10</b>
1.6	<b>LXR-ligands</b>	<b>10</b>
1.6.1	Endogenous LXR ligands	11
1.6.2	Synthetic LXR-ligands	11
1.7	<b>Natural compounds in drug discovery</b>	<b>11</b>
1.7.1	Limonoids	12
1.7.2	Flindissone as LXR modulator	13
<b>2</b>	<b><i>Aim of the study</i></b>	<b>16</b>
<b>3</b>	<b><i>Materials</i></b>	<b>17</b>
3.1	<b>Product and supplier information</b>	<b>17</b>
3.2	<b>Cell culture media and supplements</b>	<b>18</b>
3.3	<b>Luciferase reporter gene assay</b>	<b>20</b>
3.4	<b>Mammalian one-hybrid assay: GAL4/UAS luciferase assay</b>	<b>22</b>
3.5	<b>Western blot</b>	<b>22</b>
3.6	<b>qPCR</b>	<b>25</b>
<b>4</b>	<b><i>Methods</i></b>	<b>26</b>
4.1	<b>Cell culture</b>	<b>26</b>
4.1.1	HEK293	26
4.1.2	THP-1	26
4.1.3	HepG2	27
4.1.4	Freezing	27
4.1.5	Thawing	28
4.2	<b>Luciferase reporter gene assay in HEK293 cells</b>	<b>28</b>
4.3	<b>Mammalian one-hybrid assay: GAL4 luciferase assay</b>	<b>31</b>
4.4	<b>Differentiation of THP-1 monocytes into THP-1 macrophages</b>	<b>32</b>
4.5	<b>Western blot</b>	<b>33</b>
4.6	<b>RT-qPCR</b>	<b>35</b>

4.7	Statistics .....	38
5	<b>Results .....</b>	<b>39</b>
5.1	Flindissone can activate the full-length receptor LXR $\alpha$ .....	39
5.2	Activation of LXR $\alpha$ and LXR $\beta$ via LBD .....	42
5.3	Cotreatment experiments .....	44
5.4	Flindissone enhances ABCA1 and ABCG1 in THP-1 macrophages .....	46
5.5	The effect of flindissone on SREBP1 gene expression in HepG2 cells.....	48
5.6	The effect of flindissone on the LDLR gene expression in HepG2 cells .....	49
6	<b>Discussion .....</b>	<b>51</b>
7	<b>Appendix.....</b>	<b>54</b>
7.1	Abbreviation.....	54
7.2	Figures.....	57
7.3	Tables .....	62
8	<b>Literature .....</b>	<b>63</b>
9	<b>Acknowledgements .....</b>	<b>71</b>

# 1 Introduction

## 1.1 Atherosclerosis

In general, the term atherosclerosis refers to chronic inflammation of the arterial walls together with an accumulation of lipids in the inner layer of the arteries, the tunica intima. Atherosclerotic cardiovascular disease (ASCVD) and its clinical manifestations, such as ischemic stroke and myocardial infarction, represent the leading causes of death worldwide. Over 17 million people died from ASCVD and its associated sequelae in 2015. This accounts 31 % of total deaths worldwide. In 2015, the *Global Burden of Disease* project found that more than 75 % of all ASCVD deaths worldwide, primarily affect low- and middle-income countries. This is a consequence of limited access to a functioning and equitable healthcare system, which should serve to educate, diagnose, and treat atherosclerosis.<sup>1-4</sup>

The word atherosclerosis is derived from the Greek word "atheros", which means mucus and alludes to the visual appearance of the lipids inside an atherosclerotic plaque. Risk factors that may trigger atherosclerosis include tobacco use, obesity, hypertension, physical inactivity, high alcohol consumption, diabetes mellitus and dyslipidemia.<sup>5</sup> There is ample evidence that an excess of the cholesterol-rich low density lipoprotein (LDL), as well as other apolipoprotein B containing lipoproteins such as very low density lipoprotein (VLDL), intermediate density lipoprotein (IDL), and lipoprotein a (Lp(a)), is associated with the development of ASCVD.<sup>6</sup>

### 1.1.1 Development of atherosclerosis

Within atherogenesis a persistent stenosis occurs together with a chronic inflammatory process of the vessels, which is characterized by endothelial dysfunction and, above all, by an accumulation of LDL and the activation of immune cells.<sup>6-8</sup> Arterial walls consist of three layers, the tunica intima, tunica media and tunica externa or adventitia. The tunica intima consists of a single-layer endothelium and the basal membrane and is in constant contact with circulating blood. The tunica media contains smooth muscle cells (SMC) embedded in an extracellular matrix consisting of elastin, collagen, and other

macromolecules. The tunica externa contains mast cells, nerve endings, the vasa vasorum and microvessels.<sup>9-11</sup>

Atherogenesis begins usually in childhood and adolescence and leads to a vessel wall thickening in middle age.<sup>6</sup> Even before LDL is deposited in the intima, physiological adaptations cause the intima to vary in thickness in different arterial segments. Mechanical influences, such as fluctuating shear stress lead to intimal hyperplasia and therefore to the accumulation of SMCs and proteoglycans. These predisposed sections are later particularly susceptible to the development of atherosclerotic plaques by retention of LDL in the presence of a hyperlipidemia.<sup>10,12</sup> Endothelial dysfunction is also triggered by hypertension, diabetes, smoking, obesity, and hypercholesterolemia. The above risk factors cause changes in the permeability of the endothelial layer to LDL and LDL particles begin to accumulate in the intima. In the intima, LDL can undergo oxidative modifications. Oxidized LDL (oxLDL) may arise enzymatic, by, for example, myeloperoxidases or lipoxygenases, or nonenzymatic, by formation of reactive oxygen species, by activated endothelial cells or macrophages. Often, modified LDL is just considered as a ligand for the scavenger receptor, but oxLDL particles are the main components that contribute the development of inflammation and can trigger both, innate and adaptive immune responses.<sup>13-15</sup>

Leukocytes, and especially monocytes, can accumulate in the subendothelial space via adhesion molecules expressed by endothelial cells (such as vascular cell adhesion molecule; VCAM). In the hyper lipidic environment of the intima, monocytes can differentiate into tissue-macrophages, which express scavenger receptors that can uptake lipoproteins (especially oxLDL) and develop into foam cells and fatty streaks, the precursors of atheromas. The differentiation of monocytes into macrophages is mainly stimulated by macrophages colony-stimulating factor (M-CSF).<sup>3,15,16</sup> The somewhat oddly chosen term foam cells, stems from the microscopic appearance of lipid-laden macrophages.<sup>11</sup>

The recruitment of SMCs from the tunica media into the tunica intima is also a significant factor in atheroma formation. SMCs that have accumulated in the intima, produce extracellular matrix molecules, such as collagen and elastin, which form the components of the fibrous cap.<sup>11</sup> The steady growth of atherosclerotic plaques causes stenosis, which impairs the blood flow. This can result in an oxygen deficiency in the tissue, leading to ischemia. In most cases, the atherosclerotic plaque gets physically destroyed over the time. Occlusive thrombi are the reasons of the clinical endpoints, such as ischemic insult,



acute coronary syndrome, or stroke. The so-called vulnerable plaques usually have large lipid cores and a thin fibrous cap, whereas plaques with limited lipid accumulation and thick fibrous cap are called stable plaques, which are less susceptible to rupture.<sup>17,18</sup> Damage of the plaque releases procoagulant material, such as tissue factor, from the plaque interior. An exposure of tissue factor to flowing blood triggers the coagulation cascade. Thrombin is produced and thrombin in turn promotes cleavage of fibrinogen to fibrin, which coats the surface of the exposed plaque.<sup>19</sup> Normally, healthy endothelium has anticoagulant and fibrinolytic properties and can balance procoagulant factors. Plaque rupture causes a loss of the antithrombotic effects of healthy endothelium, because after rupture the endothelium has an eroded surface and is no longer fully functional.<sup>20</sup>

The discovery of the first statin mevastatin from the fungus *Penicillium citrinum* was a milestone in the treatment of ASCVD. Statins inhibit 3-hydroxy-3-methylglutaryl-CoA reductase (HMG-CoA), the rate-limiting enzyme in cholesterol biosynthesis. According to the European Society of Cardiology and the European Atherosclerosis Society, statin therapy remains the treatment of choice for hypercholesterolemia. A reduction in LDL-cholesterol (LDL-C) with statins as primary or secondary prevention is associated with a reduction in ASCVD mortality and morbidity. However, there are still patient groups, such as individuals with familial hypercholesterolaemia (FH) or patients with statin intolerance, who would require alternative or combined treatment. Furthermore, statins have little to no effect on elevated Lp(a) levels, which is a serious risk factor for developing atherosclerosis. Fibrates, ezetimibe and, in severe cases, proprotein convertase subtilisin/kexin type 9 (PCSK9) inhibitors are also used for the primary prevention of atherosclerosis.<sup>5,11,13,21</sup> The detailed discussion of these is beyond the scope of this work, but for a global epidemic such as atherosclerosis, the search for novel treatments should not stand still.

## 1.2 Nuclear receptors

Nuclear receptors (NR) are ligand-activated transcription factors. In humans 48 different genes are known that encode for NR. NRs represent a therapeutic target in the treatment

of various diseases such as diabetes, cancer, reproduction, atherosclerosis, or inflammation.<sup>22,23</sup>

NR can be divided into four mechanistic subtypes. NR such as LXR and RXR belong to type II and are localized in the nucleus regardless of the presence or absence of their ligand. In the absence of a ligand, transcriptional corepressors are bound to the ligand-binding domain (LBD) of the NR. These recruit transcriptional complexes containing, for example, histone deacetylases (HDAC), which can remove acetyl groups from lysine residues of histones, causing the lysines to become positively charged and interact closely with the negatively charged DNA, generating a compact condensed chromatin structure which repress gene expression. If a ligand now comes into play, the corepressor complex dissociates, and coactivator complex is recruited. These possess histone acetyltransferase (HAT) activity, allowing the condensed chromatin to loosen and gene transcription to occur.<sup>24</sup>

NR can either act as homodimers, like steroid receptors, or they act as heterodimers, such as RXR and LXR. Most type II NR form heterodimers with RXR. NR occurring as monomers belong in most cases to the orphan receptors, where the endogenous ligands have not been identified yet.<sup>1,23</sup>

### 1.2.1 Structure of nuclear receptors

Sequence analyses of different NR revealed a highly conserved structure that can be divided into six functional domains. The ligand-independent activation function-1 (AF-1), also called A/B domain, is located at the amino-terminal end. AF-1 is important for interaction with coregulators and other transcription factors. The DNA-binding domain (DBD) or C domain, mediates binding of the receptor to the response element (RE) in the promoter region of the target genes. The C domain is the most conserved domain and is rich of cysteine and basic amino acids. The D domain is located between the DBD and the ligand-binding domain (LBD) and is referred as the hinge domain. It is characterized by its low degree of conservation. The ligand-dependent activation function-2 (AF-2), LBD or domain E, contains the ligand binding pocket. Coactivators and corepressors also bind to this domain and determine the transcriptional activity of the NR. Region F is present in only a few NRs and usually plays a somewhat minor role.<sup>1,22,25</sup>

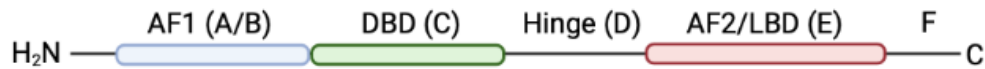


**Figure 1** Most NR consist of six functional domains: the N-terminal ligand-independent activation function-1 (AF-1), the highly conserved DNA-binding domain (DBD), between the DBD and ligand-binding domain (LBD) is the hinge domain located, the ligand-dependent activation function-2 (AF2) and the highly variable F domain located at the C-terminal end. Adopted and modified from: Mangelsdorf et al., 1995<sup>1</sup>. Created with BioRender.com

### 1.2.2 Mechanism of action of nuclear receptors

The LBD of all NR exhibits a highly conserved tertiary structure with a globular domain consisting almost exclusively of  $\alpha$ -helices. Most ligands bind into the LBP (ligand-binding pocket) of the globular domain. Within the globular domain, there are 11  $\alpha$ -helices and helix 12 (H12) forms a "lid" that can move at the entrance of the LBP. How H12 positioning is ligand-dependent and critical for the formation of a coactivator-binding surface in the LBD, which is then again responsible for the recruitment of coactivator proteins. In the absence of a ligand, H12 remains highly mobile. As soon as a ligand comes into play, H12 is stabilized over the globular domain and a hydrophobic pocket is formed. This surface recognizes a very characteristic motif for coactivator proteins, called NR-box or LXXLL motif (L=leucine, X=any amino acid). Corepressors also have a very typical motif sequence for LBD recognition. This is very similar to the sequence of coactivators and is called the CoRNR box. When an agonist binds, the position of H12 is aligned to exclude binding of the CoRNR box of corepressors.<sup>25-27</sup>

## 1.3 Liver X receptor

The LXR is a ligand-activated transcription factor and a member of the NR superfamily. In the mid-1990s, the two isotypes LXR $\alpha$  and LXR $\beta$  were identified. With the identification of oxysterols as endogenous ligands, the potential importance of LXR in cholesterol metabolism was recognized. LXR $\alpha$  and LXR $\beta$  show a 77% sequence homology in their DBD and LBD but are differentially expressed in different tissues. LXR $\alpha$  is predominantly expressed in highly metabolic tissues, such as liver, intestine, and adipose tissue, whereas LXR $\beta$  is expressed ubiquitously. Both isotypes form obligate heterodimers with RXR and bind together to a specific DNA recognition sequence, called

LXR response element (LXRE). The recognition sequence LXRE consists of different repeats of AGGTCA separated by four nucleotides and located in the promoter region of the target genes. In the absence of a ligand, the lysine residues of the histones are deacetylated and LXR is constitutively bound to RXR. When a ligand binds, the corepressor complexes, such as the silencing mediator of retinoic acid and thyroid hormone receptor (SMRT) or nuclear receptor co-repressor (NCoR) are released and the recruitment of coactivators such as histone acetyltransferase p300 (HATp300) takes place. This results in the loosening of condensed chromatin and the initiation of target gene transcription. The LXR/RXR heterodimer can be transcriptionally activated by LXR or RXR ligands and is therefore referred to as a permissive heterodimer.<sup>28-31</sup>

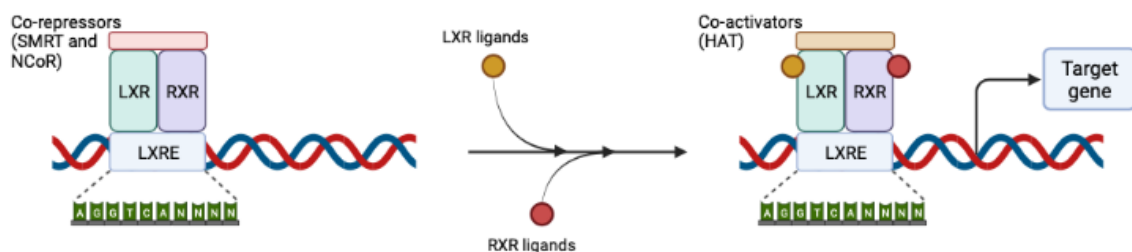


**Figure 2 Transcriptional induction of LXR.** In the absence of a ligand, the transcription of the target genes is repressed by corepressors, such as silencing mediator of retinoic acid and thyroid hormone receptor (SMRT) or nuclear receptor co-repressor (NCoR). If the LXR/RXR heterodimer is now activated with a ligand, this causes a conformational change of the receptor: the corepressor is released, and a coactivator is recruited. Created with BioRender.com

Cholesterol is a component of all cell membranes and serves as a precursor for the endogenous production of steroid hormones and bile acids. Excess cholesterol can lead to ASCVD and consequently to the clinical manifestations of these. The LXR has a significant role in cholesterol homeostasis and is a master regulator of genes involved in processes such as intestinal cholesterol absorption, cholesterol biosynthesis and uptake in the liver, cholesterol elimination through the conversion of cholesterol into bile acids, HDL formation and reverse cholesterol transport.

## 1.4 LXR target genes

### 1.4.1 LXR activation in the intestine

ATP binding cassette subfamily G member 5 (ABCG5) and ATP binding cassette subfamily G member 8 (ABCG8) are two “half” ABC transporter, which form a heterodimer in the apical membrane of enterocytes and play an important role in cholesterol excretion in the intestine. LXR agonists can increase expression of these ABC transporters and promote cholesterol efflux in enterocytes into the intestinal lumen, resulting in less cholesterol absorption and increased cholesterol excretion through the feces. The dietary cholesterol is absorbed primarily by NPC1 like intracellular cholesterol transporter 1 (NPC1L1). NPC1L1 is a protein that is expressed in the small intestine in the apical membrane of enterocytes and is the molecular target of the cholesterol absorption inhibitor, ezetimibe. By activating LXR, NPC1L1 expression gets downregulated, and this leads to decreased intestinal cholesterol absorption and increases fecal cholesterol excretion. In conclusion LXR activation in the intestine reduces cholesterol absorption and promotes fecal cholesterol excretion by up-regulating the transcription of ABCG5 and ABCG8 on the one hand and by down-regulating the transcription of NPC1L1 on the other hand. Furthermore, the LXR activation promotes ATP binding cassette subfamily A member 1 (ABCA1) expression in the intestine and therefore HDL formation and reverse cholesterol transport (RCT) to the liver, which will be discussed in more detail later in the work.<sup>32-34</sup>

### 1.4.2 LXR activation promotes cholesterol excretion in the liver

Cytochrome P450 family 7 subfamily A member 1 (CYP7A1) is the rate-limiting enzyme in the conversion of bile acid into cholesterol. CYP7A1 was identified as one of the first LXR target genes. LXR agonists increase CYP7A1 expression, resulting in increased conversion of cholesterol into bile acid, which can be excreted via the bile duct. In the liver, ABCG5/G8 is also an LXR target; increased expression of the heterodimer enhances hepatobiliary cholesterol excretion.<sup>35,36</sup>

### 1.4.3 The role of LXR in reverse cholesterol transport

With the discovery of the Tangier disease, the importance of ABCA1 in cholesterol metabolism gained attention. Due to mutations in the gene encoding for ABCA1, patients

suffering from Tangier disease have reduced HDL levels and increased cholesterol exposure in peripheral tissues and therefore an increased risk to develop atherosclerosis.<sup>37</sup> ABCA1 and ABCG1 belong to the ABC superfamily, which use adenosine triphosphate (ATP) as an energy source to transport substances across a membrane. Both ABC transporters mediate the efflux of cholesterol and phospholipids to lipid-poor apolipoproteins. The major difference between the two transporters is that ABCG1 transports cholesterol to HDL2 and HDL3, whereas ABCA1 transports cholesterol primarily to lipid-free ApoA1.<sup>38</sup>

LXR agonists can activate ABCA1 especially in macrophages and in the small intestine, resulting in the stimulation of the reverse cholesterol transport (RCT). The RCT is a pathway consisting of several steps that ensures that excess cholesterol from the peripheral tissue is transferred to HDL and transported back to the liver for bile acid synthesis and excretion. The first step of RCT is the cellular cholesterol efflux, which is mediated primarily by ABCA1. In this step free cholesterol is transferred to ApoA1 and/or pre- $\beta$  HDL. Thereafter, cholesterol is esterified by lecithin-cholesterol acyltransferase (LCAT) and shifted to the center of HDL particles. Mature HDL particles are formed through several intermediate enzymatic steps where cholesterol, phospholipids and apolipoproteins are exchanged. The mature HDL particles are then taken up for cholesterol degradation by the liver through the HDL receptor, SR-B1. LXR agonists can also induce ABCG1 expression and therefore promote cellular cholesterol efflux and RCT.<sup>39-41</sup>

#### 1.4.4 The importance of LXR in cholesterol uptake and biosynthesis in the liver

The liver is one of the key organs when it comes to cholesterol biosynthesis and cholesterol degradation. The liver takes up cholesterol from plasma via LDL through the LDLR. Sterol regulatory element-binding protein 2 (SREBP2) and LXR represent regulators for cholesterol synthesis and cholesterol uptake in the liver. LXR promotes the elimination of excess cholesterol, whereas SREBP2 (one of the three isoforms of SREBP) can respond to low cholesterol levels and promote cholesterol biosynthesis and uptake. SREBP2 is anchored in the membrane of the endoplasmic reticulum. The actual cholesterol sensor is a protein called sterol regulatory element-binding protein cleavage-activating protein (SCAP), which is bound to SREBP2 with its C-terminal domain. At low cholesterol concentrations, SREBP2 is not fixed in the endoplasmic reticulum, and is instead transported to the Golgi apparatus with the help of vesicles and gets

proteolytically modified there. SREBP2 can now migrate into the nucleus as a transcription factor and bind to the steroid response element (SRE) of several target genes and initiate the transcription of genes involved in cholesterol biosynthesis and the transcription of the LDLR, which promotes cholesterol uptake. If conditions change and intracellular cholesterol levels are elevated, SCAP binds to a protein called Insig, which prevents SREBP from detaching from the complex with SCAP and being transported to the Golgi by vesicles. This mechanism has the opposite effect, suppressing the expression of target genes involved in cholesterol biosynthesis and LDL uptake.<sup>42-44</sup>

Peet et al. 1998 found that LXR $\alpha$ -deficient mice fed a chow diet, showed increased expression of SREBP2. As mentioned above, SREBP2 then in turn increases the expression of genes involved in cholesterol biosynthesis, such as HMG-CoA synthase, HMG-CoA reductase, or other enzymes of the mevalonate pathway like farnesyl diphosphate synthase or squalene synthase.<sup>36</sup>

When a LXR agonist activates LXR, the opposite effect can be observed; LXR increases the expression of IDOL (also called myosin regulatory light chain interacting protein (MYLIP)) via an SREBP-independent mechanism. IDOL is an E3 ubiquitin protein ligase. This can ubiquitylate and degrade the LDLR, and thus less LDL is taken up from plasma via the LDLR into the liver, which can increase plasma LDL levels. Ishimoto et al. 2006 found that the LDLR could also be a direct target gene of LXR $\alpha$ . Activation of LXR $\alpha$  increases LDLR expression in an SREBP2 independent manner. The exact reason why LDLR gene expression is directly upregulated by LXR $\alpha$  on the one hand and on the other hand, activation of LXR degrades LDLR via increased expression of IDOL, resulting in the exact opposite effect, is still unclear.<sup>45,46</sup>

#### 1.4.5 The problem of LXR activation in fatty acid metabolism

Activation of LXR in fatty acid metabolism leads to an increased expression of target genes involved in *de novo* lipogenesis. Therefore, higher number of triglycerides are produced, which leads to hypertriglyceridemia and consequently to liver steatosis. In many studies, this effect has been explained by the direct upregulation of SREBP1c by LXR. SREBP1c is the dominant SREBP1 isoform in the liver, which increases the transcription of lipogenic genes such as fatty acid synthesis (FAS), acetyl-CoA-carboxylase (ACC) and stearyl-CoA desaturase-1 (SCD1). In addition, there are some publications in which LXR is directly involved in the upregulation of FAS and SCD1 via LXRE in their promoter region.<sup>47-49</sup>

## 1.5 Selective LXR modulators

As discussed in the chapter "LXR Target Genes", LXR activation has many beneficial effects on cholesterol metabolism and serves therefore as a potential therapeutic target in the treatment of ASCVD. However, most identified LXR agonists can also upregulate SREBP1c expression in the liver, resulting in the side effect of hypertriglyceridemia and consequently in hepatic steatosis.

Due to this fact, increased research for tissue-specific or gene-specific next generation LXR modulators started in the last decade. The ideal idea would imply being able to identify LXR modulators that exhibit, for example, tissue-specific activation, such as specificity for LXR activation in macrophages versus a LXR activation in the liver. Another possibility would be, if LXR agonists would show some gene selectivity, such as increased activation of ABCA1 and ABCG1 without activation SREBP1c and thereby stimulating the desired cholesterol efflux and RCT without developing hypertriglyceridemia from SREBP1c upregulation.

Modulators, which exhibit tissue or target gene specificity, can possibly induce an individual conformation within the LBD of NR, resulting in a different motif sequence in the LBD, that influences the recruitment of coactivators and corepressors. Likewise, different cell types express different amounts of coactivators or corepressors. This variation in the ratio of coactivators and corepressors in each cell type could explain the ability of some ligands to modulate in a tissue-specific manner.<sup>50,51</sup>

Currently, the trend in LXR research is towards the search for selective LXR $\beta$  agonists, as it is often postulated in the literature that only LXR $\alpha$  is involved in the increased expression of SREBP1c in the liver.<sup>52</sup> It is to note that LXR $\alpha$  is the dominant LXR isotype in the liver and therefore naturally participates more in the increased SREBP-1c expression.<sup>53</sup>

## 1.6 LXR-ligands

The focus of this chapter is primarily on the description of the four LXR agonists GW3965, T0901317, 22-R-hydroxycholesterol and flindisone. These were investigated in the experimental section for their ability to regulate LXR target genes. However, there



are nowadays numerous synthetic LXR ligands, as well as LXR ligands of natural origin.<sup>54</sup>

#### 1.6.1 Endogenous LXR ligands

Oxysterols are oxygenated cholesterol derivatives and represent endogenous LXR ligands. Oxysterols can either be provided endogenously via enzymatic or non-enzymatic reactions or they can be provided via the diet.<sup>55</sup> Known endogenous LXR ligands would be 22(R)-hydroxycholesterol, 24(S)-hydroxycholesterol, 24(S),25-epoxycholesterol and 27-hydroxycholesterol. All mentioned endogenous ligands can activate the two LXR isotypes.<sup>56,57</sup>

In 1996 Janowski et al. screened oxysterols for the first time for their ability to activate LXR $\alpha$ . Through initial screening of endogenous ligands in the GAL4/UAS reporter gene assay, the group found that the endogenous ligand 22-R-hydroxycholesterol (17-(3-hydroxy-6-methylheptan-2-yl)-10,13-dimethyl-2,3,4,7,8,9,11,12,14,15,16,17-dodecahydro-1H-cyclopenta[a]phenanthren-3-ol) can activate the LXR $\alpha$  most strongly among the oxysterols (tested at 10  $\mu$ M in CV-1 cells).<sup>56</sup>

#### 1.6.2 Synthetic LXR-ligands

In the early 2000s, probably the two most prominent LXR agonists were synthesized, which seemed promising in using LXR as a target in the treatment of atherosclerosis. T0901317 (N-[4-(1,1,1,3,3,3-hexafluoro-2-hydroxypropan-2-yl)phenyl]-N-(2,2,2-trifluoroethyl)benzenesulfonamide)) and GW3965 (2-[3-[3-[[2-chloro-3-(trifluoromethyl)phenyl]methyl-(2,2-diphenylethyl)amino]propoxy]phenyl]acetic acid) are potent nonsteroidal LXR $\alpha$  and LXR $\beta$  agonists. Both compounds couldn't enter clinical trial because of the increased risk for the development of hypertriglyceridemia, due to the increased transcription of SREBP1c.<sup>47,58</sup>

### 1.7 Natural compounds in drug discovery

Natural compounds provide a promising source for the development of new drugs. They can either be isolated directly and used therapeutically or can serve as inspiration for novel synthetic compounds.<sup>59</sup>

Since the beginning of human history, people were dependent on plants to treat their physical ailments. 2600 BCE in the advanced civilization of Mesopotamia, 1000 plants used as medicine were documented.<sup>60</sup> A large percentage of the world's population is still dependent on plant-derived traditional medicine in treating of primary health care needs. This shows that in many parts of the world plants are still the only access for alleviating or curing diseases and are therefore indispensable.<sup>61</sup>

The isolation of morphine from opium in 1805 by Friedrich Sertürner marked the beginning of modern drug discovery. Not only the isolation of morphine was world-changing, morphine was also the first compound of natural origin that served as a source for the derivatization of other compounds.<sup>62</sup>

After the discovery of penicillin, a very successful era of natural-product driven drug discovery was followed, but a significant decline took place around 1990. With the discovery of high throughput screening (HTS), the pharmaceutical industry minimized its interest and therefore the investment in natural product-driven drug discovery. The rationale for this was that natural compounds were less suitable for HTS due to their complexity and heterogeneity.<sup>63</sup> Furthermore, the industry's interest in natural products became smaller and smaller due to the often-limited access to the primary product. A prominent example of this is paclitaxel, which was traditionally isolated from *Taxus brevifolia*. To treat 500 patients with 1 kg of paclitaxel from *Taxus* species would require 300 100-year-old trees. Another disadvantage of natural compounds is the difficulty of isolating and purifying the active compound in a complex multicomponent mixture.<sup>63,64</sup> Natural compounds are usually much more chemically complex than synthetic compounds and have usually a higher molecular weight. Natural compounds are produced by living organisms and often exhibit an improved pharmacokinetics due to the evolutionary pressures to which they have been subjected.<sup>65</sup>

Even though natural compounds often have many disadvantages, the past has shown us that probably the greatest achievements in pharmacy come from nature or are inspired by it and the search for new compounds should not end yet.

#### 1.7.1 Limonoids

Limonoids are secondary metabolites, and the word “limonoid” is derived from the first isolated limonoid, limonoin. Limonoids are highly oxygenated triterpenoids and are found mostly in the plant families Rutaceae and Meliaceae. In the literature, however,

limonoids are usually referred to as tetraterpenoids because the cyclization of the 17 $\beta$ -furan ring results in a loss of the four terminal carbon atoms in the side chain.<sup>66,67</sup>

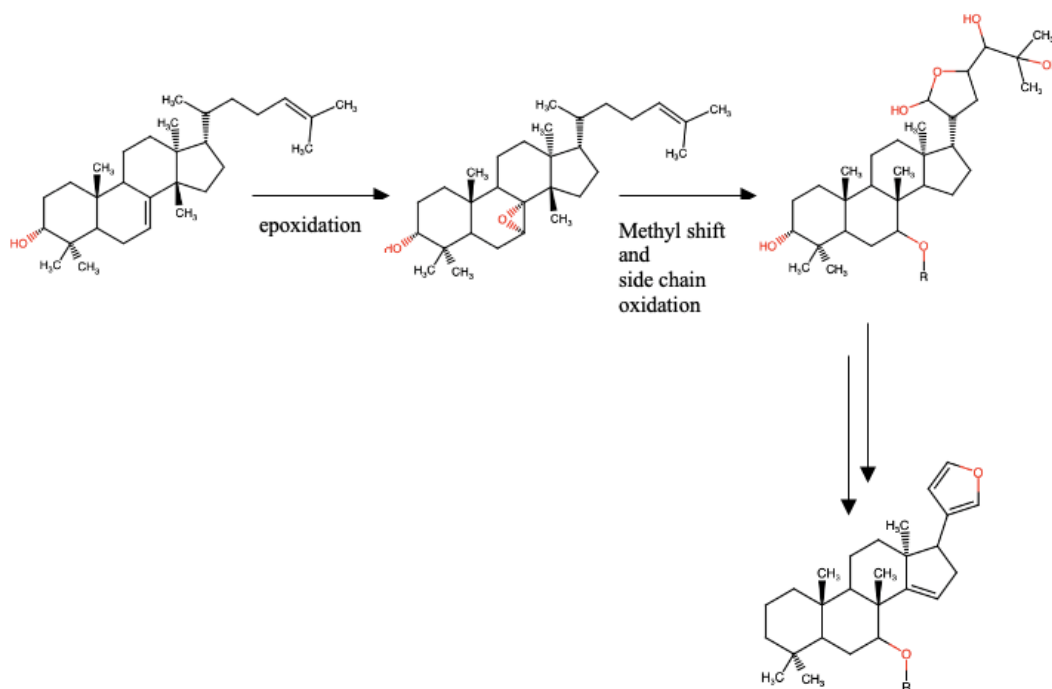


**Figure 3 Cyclization of the 17 $\beta$ -furan ring.** Adopted and modified from: Q. Tan and X. Luo 2011<sup>67</sup>

Limonoids are characterized by their diversity of the chemical structure and biological activity. They are primarily known because of their insecticidal effect, but they also show anticancer, antiviral, antimalarial and antibacterial activity.<sup>68</sup>

### 1.7.2 Flindissone as LXR modulator

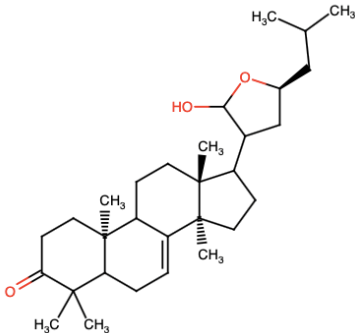
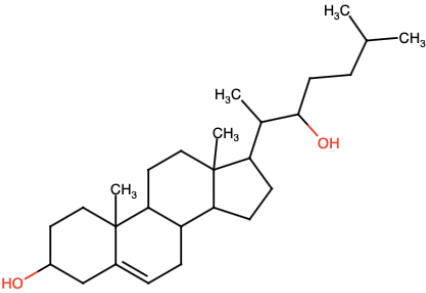
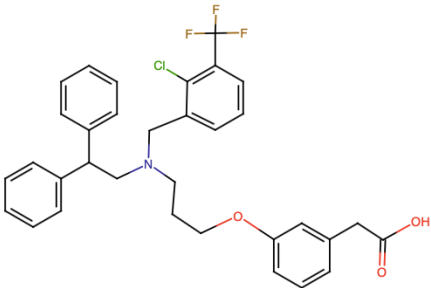
Flindissone (5R,9R,10R,13S,14S,17S)-17-[(2R,3S,5R)-2-hydroxy-5-(2-methylpropyl)oxolan-3-yl]-4,4,10,13,14-pentamethyl-1,2,5,6,9,11,12,15,16,17-decahydrocyclopenta[a]phenanthrene-3-one) is a limonoid which was first isolated from *Aucoumea klaineana* (Burseraceae) in 1989.<sup>69</sup> In the literature, three other plants have been mentioned from which flindissone has been isolated so far: leaves and twigs of *Luvunga sarmentosa* (Rutaceae),<sup>70</sup> aerial parts of *Guarea guidonia* (Meliaceae)<sup>71</sup> and fruits of *Paramignya monophylla* (Rutaceae).<sup>72</sup> The flindissone used in this work is derived from the leaves of *Trichilia prieuriana* of the Meliaceae family.

Plants of the genus *Trichilia* grow mainly in tropical and subtropical areas such as sub-Saharan Africa and South America.<sup>73</sup> The use of *Trichilia prieuriana* is hardly reported,

but antibacterial effects have been observed and Pagna et al. 2021 wrote in their publication about the traditional use of the plant against malaria, syphilis, trypanosomiasis, pneumonia and cold.<sup>74</sup>

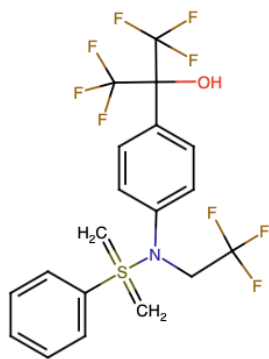
Limonoids are structurally very diverse compounds and often no uniform classification is used in the literature. In 2012, Tan and Luo wrote a detailed review of all known limonoids in the Meliaceae family and attempted to classify them into groups. Thus, there are three major groups of limonoids in the Meliaceae family: ring-seco, intact rings and rearranged limonoids. Flindissone was not mentioned in this publication, but structurally it would belong to the intact ring group.<sup>67</sup>

**Table 1 Structure of LXR agonists**

<i>Name</i>	<i>Structure</i>	<i>Reference</i>
Flindissone		69
22-R-hydroxycholesterol		56
GW3965		58

T0901317

58



## 2 Aim of the study

The aim of this study was to investigate flindissone for its regulatory abilities on LXR target genes in cholesterol metabolism and thereby find a new agent for the treatment of ASCVD.

Whether and to what extent flindissone can activate the LXR $\alpha$  and/ or LXR $\beta$  was determined by testing different flindissone concentrations in the luciferase reporter gene assay in HEK293 cells. From the results, a dose-response curve was generated with the corresponding EC50 values.

The aim was to get a first indication whether flindissone is a gene- or tissue-selective LXR modulator and can upregulate the ABC transporters ABCA1 and ABCG1 in THP-1 macrophages, thereby showing a positive effect on cholesterol efflux, but without an inducing effect on SREBP1c expression in HepG2 cells.

Furthermore, the influence of flindissone on LDLR gene expression in HepG2 cells was determined to obtain conclusions on LDL uptake in the liver.

### 3 Materials

#### 3.1 Product and supplier information

**Table 2 Supplier information**

<i>Cell culture media</i>	
DMEM with 4.5 g/l glucose without L-glutamine and phenol red	Lonza
RPMI-1640 without L-glutamine	Lonza
L-glutamine 2 mM	Lonza
Penicillin – Streptomycin	Lonza
FBS (heat inactivated at 56 °C for 30 minutes and sterile filtered)	Gibco
Trypsin (1:250), powder	Gibco
Charcoal-stripped FBS	Gibco
<i>Reagents</i>	
APS	Fluka
ATP	Sigma Aldrich
BSA	Carl Roth
Cholesterol-water soluble	Sigma Aldrich
Coenzyme A (CoA) trilithium salt	Sigma Aldrich
Complete	Roche Diagnostics AG
DMSO	Sigma Aldrich
Dithiothreitol (DTT)	Fluka
D-luciferin	Synchem
EDTA	Carl Roth
Glycine	Carl Roth
H <sub>2</sub> O <sub>2</sub>	Carl Roth
IGEPAL CA-630	Sigma Aldrich
Luminol	Sigma Aldrich
5x lysis buffer	Promega

Rotiphorese (PAA)	Carl Roth
ROTI®Quant, 5x	Carl Roth
PMA	Sigma Aldrich
PMSF	Sigma Aldrich
Precision Plus Protein™ Protein Standards	Bio-Rad
p-Coumaric Acid	Sigma Aldrich
SDS	Carl Roth
SYBR Safe	Invitrogen
TEMED	Carl Roth
Tris-Base	Carl Roth
Tris-HCl	Carl Roth
Triton X-100	Sigma Aldrich
Tween 20	Carl Roth

**Table 3 Compounds supplier information**

Compounds	
Flindissone	The University of Ngaoundere; Faculty of science
GW3965	Sigma Aldrich
T0901317	Sigma Aldrich
22-R-hydroxycholesterol	Sigma Aldrich

### 3.2 Cell culture media and supplements

**Table 4 Cell culture media and supplements**

<i>Trypsin/EDTA in PBS</i>	
Trypsin + EDTA	0.05 % + 0.02 %
<i>PBS (pH 7.4)</i>	
NaCl	123 mM



NH <sub>2</sub> HPO <sub>4</sub>	10.4 mM
KH <sub>2</sub> PO <sub>4</sub>	3.16 mM
In ddH <sub>2</sub> O	1000 ml
<i>DMEM completed growth medium</i>	
DMEM (4.5 g/l glucose) without L-glutamine and phenol red	500 ml
Penicillin	100 U/ml
Streptomycin	100 µg/ml
FBS	10 %
L-glutamine	2 mM
<i>RPMI-1640 completed growth medium</i>	
RPMI-1640 without L-glutamine	500 ml
Penicillin	100 U/ml
Streptomycin	100 µg/ml
FBS	10 %
L-glutamine	2 mM
<i>Stripped medium</i>	
DMEM (4.5 g/l glucose) without L-glutamine and phenol red	500 ml
Penicillin	100 U/ml
Streptomycin	100 µg/ml
L-glutamine	2 mM
Charcoal-stripped FBS	5 %
<i>2.5 % FBS/serum-free DMEM with 20 µg/ml cholesterol-water soluble</i>	
DMEM (4.5 g/l glucose) without L-glutamine and phenol red	500 ml
Penicillin	100 U/m
Streptomycin	100 µg/ml
FBS	2 %
L-glutamine	2 mM
Cholesterol-water soluble	10 mg/ml
Cholesterol-water soluble was added immediately before usage	

<i>0.1 % BSA/serum-free DMEM</i>	
DMEM (4.5 g/l glucose) without L-glutamine and phenol red	500 ml
Penicillin	100 U/ml
Streptomycin	100 µg/ml
L-glutamine	2 mM
BSA	2 %
BSA was added immediately before usage	
<i>Freezing medium</i>	
DMEM completed growth medium	70 %
DMSO	10 %
FBS	20 %
Mixed immediately before usage	

**Table 5 Supplier information of used cell lines**

<i>Cell lines</i>	
HEK293	ATCC
HepG2	ATCC
THP-1	ATCC

### 3.3 Luciferase reporter gene assay

**Table 6 Reagents, plasmids and buffers used in the luciferase reporter gene assay**

<i>Transfection mixture (Total 1.5 ml/15 cm plate)</i>	
CaCl <sub>2</sub>	94 µl
2x HBS	750 µl
ddH <sub>2</sub> O	To 1.5 ml
+ Plasmids (see table below)	
Mixed immediately before usage	

<i>HBS pH=7.1</i>	
NaCl	280 mM
Na <sub>2</sub> HPO <sub>4</sub> x 2 H <sub>2</sub> O	1.5 mM
HEPES	50 mM
<i>Plasmid preparation</i>	
BL21(DE3) Singles Competent Cells	Sigma
PureYield™ Plasmid Midiprep System	Promega
<i>Full length receptors</i>	
Human LXRα in pCMV vector	Missouri S&T cDNA Resource Center
Human LXRβ in pcDNA3.1+vector	Missouri S&T cDNA Resource Center
<i>Response elements</i>	
Human ABCA1 promotor (-703/-38) in pGL4.14 vector	Ira G. Schulman (University of Virginia)
<i>Plasmids ratio for transfection mixture</i>	
LXRα : ABCA1 : eGFP	3 µg : 6 µg : 3 µg
LXRβ : ABCA1 : eGFP	3 µg : 6 µg : 3 µg
<i>Luciferase lysis buffer</i>	
5x lysis buffer	1x
CoA	270 µM
DTT	1 mM
DTT and coenzyme A were added immediately before use	
<i>For TECAN measurments</i>	
<i>Injector A: ATP-solution</i>	
ATP (sterile-filtered)	3.7 mM
Tricine	2 mM
MgCl <sub>2</sub>	21.5 mM
<i>Injector B: Luciferin-solution</i>	
Luciferin	32 mg/ml
Tricine	21 mM

### 3.4 Mammalian one-hybrid assay: GAL4/UAS luciferase assay

**Table 7** Used plasmids in the GAL4/UAS luciferase assay

<i>NR LBD – Gal4 DBD hybrid receptors</i>	
Human LXR $\alpha$ -Gal4 in pCMX vector	Makoto Makishima (Nihon University)
Human LXR $\beta$ -Gal4 in pCMX vector	Makoto Makishima (Nihon University)
<i>Response element</i>	
UAS promotor in tk(MH1000) vector	Ronald M. Evans (Salk Institute)
<i>Plasmides ratio for transfection mixture</i>	
hLXR $\alpha$ -GAL4 : UAS-Luc : eGFP	5 $\mu$ g : 1 $\mu$ g : 3 $\mu$ g
hLXR $\beta$ -GAL4 : UAS-Luc : eGFP	5 $\mu$ g : 1 $\mu$ g : 3 $\mu$ g

Other used materials in the GAL4/UAS luciferase assay are analogous to the **Materials 3.3** of the luciferase reporter gene assay

### 3.5 Western blot

**Table 8** buffers and reagents used in the Western blot experiments

<i>RIPA buffer</i>	
Tris/HCl pH 6.8	50 mM
NP40 (Igepal)	1 % (v/v)
NaCl	500 mM
SDS	0.1 %
Sodium-desoxycholat	0.5 %
NaN <sub>3</sub>	0.05 %
<i>RIPA lysis buffer</i>	
<i>RIPA buffer</i>	
Complete	25 mM
PMSF	1 mM
NaF	1 mM
Na <sub>3</sub> VO <sub>4</sub>	1 mM

Complete, PMSF, NaF and Na <sub>3</sub> VO <sub>4</sub> were added to RIPA immediately before use	
<i>3x sample buffer</i>	
Tris/HCl pH 6.8	187.5 mM
SDS	0.2 M
Glycerol	30 %
Bromphenol blue	0.2 mM
$\beta$ -mercaptoethanol	15 %
<i>Resolving gel</i>	
Roti-Phorese Gel 30 (30 % PAA)	7.5 %
Tris/HCl pH 8.8	375 mM
SDS	0.1 %
TEMED	0.1 %
APS	0.05 %
ddH <sub>2</sub> O	To 7.5 ml
All reagents were mixed before usage	
<i>Stacking gel</i>	
Roti-Phorese Gel 30 (30 % PAA)	5 %
Tris/HCl pH 6.8	125 mM
SDS	0.1 %
TEMED	0.2 %
APS	0.1 %
ddH <sub>2</sub> O	To 3.75 ml
All reagents were mixed before usage	
<i>Electrophoresis buffer 10x</i>	
Tris-base	248 mM
Glycine	1.9 mM
SDS	35 mM
ddH <sub>2</sub> O	To 1000 ml
<i>Blotting buffer 1x</i>	
Blotting buffer 5x	20 %
Methanol	20 %
ddH <sub>2</sub> O	60 %

<i>Blotting buffer 5x</i>	
Tris-base	125 mM
Glycin	971 mM
ddH <sub>2</sub> O	To 2000 ml
<i>TBST pH 8.0 10x</i>	
Tris-base pH 8.5	248 mM
NaCl	190 mM
Tween-20	0.1 %
ddH <sub>2</sub> O	Ad 1000 ml
<i>ECL solution</i>	
Tris-base pH 8.5	1 ml
p-coumaric acid	22 µl
Luminol	50 µl
30 % H <sub>2</sub> O <sub>2</sub>	3 µl
ddH <sub>2</sub> O	9 ml
All reagents were mixed before usage	
<i>Luminol stock</i>	
Luminol	0.44 g
DMSO	10 ml
<i>p-Coumaric Acid stock</i>	
p-Coumaric acid	0.15 g
DMSO	10 ml

**Table 9 Supplier information of used antibody**

<i>Primary antibody</i>	
ABCA1	Novus Biologicals
<i>Secondary antibody</i>	
Anti-rabbit IgG, HRP linked	CST

### 3.6 qPCR

**Table 10** Used primers in the qPCR experiments

<i>Primer</i>	
Target	Sequence
Human ABCA1_P type	F: TCCCCGGTTCTGTTTTCTCC R: CGCCGTGGCTGGTCATTAA
Human ABCG1	F: CACCAGCGGCCTGGAC R: GTGCAAATGATGGAGCGACC
Human SREBPf1	F: GCTGCAGCCCCACTTCATC R: TCACCAGGGTCGGCAAAG
Human MYLIP	F: GACTGCCTCAACCAGGTGT R: GGGAGATCCGGTTTCTCAGG
Human LDLR	F: CAGCTACCCCTCGAGACAGA R: GCAGGCAATGCTTTGGTCTT
Human PPIA	F: GCCGAGGAAAACCGTGTACT R: TGTCTGCAAACAGCTCAAAGG
Human GAPDH	HS_GAPDH_1_SG QuantiTect Primer Assay

**Table 11** Reagents used in the qPCR experiments

<i>2x RT Master Mix</i>	
10x RT Buffer	2 µl
25x dNTP Mix (100 mM)	0.8 µl
10x RT Random Primers	2 µl
MultiScribe Reverse Transcriptase	1 µl
RNase Inhibitor	1 µl
RNase-free water	3.2 µl
<i>Reaction mixture</i>	
2x Green Master Mix	7.5 µl
Primers	1.5 µl
RNase-free water	4 µl
cDNA	2 µl

## 4 Methods

### 4.1 Cell culture

To avoid contamination, the following experiments were always performed under sterile conditions. A laminar air flow of HERAsafe® KS18 (Thermo Fisher) was used for this purpose. The work surface was always disinfected with 1 % hexaquart and 70 % ethanol before starting work. Incubations were always performed in a HERAcell® incubator (Thermo Fisher) at 37 °C and 5 % CO<sub>2</sub>.

#### 4.1.1 HEK293

In 1977 Frank L. Graham published the first paper about the generation of human embryonic kidney 293 cells (HEK293). The scientists transfected human embryonic kidney tissue cells with DNA fragments from human adenoviruses.<sup>75</sup>

HEK293 cells were cultured in *DMEM completed growth medium* where they form an adherent monolayer in a cell culture flask. Cells were regularly checked under the microscope (Olympus CKX31 Light Microscope; Olympus Europa GmbH) for their growth, abnormalities, and mycoplasma contamination. Once 80% confluence was achieved, cells were subcultured (usually every 48 h-72 h). The old medium was removed, and the cells were washed with 10 ml phosphate buffered saline (PBS). To detach the cells from the surface of the cell culture flask, cells were treated with 3 ml trypsin/EDTA. Once the cells detached, they were resuspended in 8 ml *DMEM completed growth medium* and an aliquot of 1 ml was taken for cell number determination, using cell counter (Vi-Cell™ XR Cell Viability Analyzer; Beckman Coulter). If a luciferase reporter gene assay was planned, HEK293 were seeded with a concentration of  $6 \times 10^6$  in 20 ml fresh medium in 15 cm Petri dishes. Another desired cells concentration was transferred to a new cell culture flask containing fresh medium.

#### 4.1.2 THP-1

THP-1 cells are a human monocytic cell line. About 40 years ago, they were isolated from a 1-year-old patient affected by acute monocytic leukemia.<sup>76</sup>



THP-1 cells were cultured in *RPMI-1640 complete growth medium*. The cells proliferate in cell suspension and exhibit a spherical single cell morphology. Typically, cells were subcultured every 48 h-72 h. In this process, the medium containing the cells were transferred to a falcon tube and centrifuged at 150 g for 4 minutes (Centrifuge Heraeus™ Multifuge 1 S-R, Thermo Fisher). The supernatant was discarded, and the cell pellet was resuspended in fresh *RPMI-1640 completed growth medium*. 1 ml of the cell suspension was collected, and the cell number was determined. For planned experiments, a desired aliquot was taken for western blot and RT-qPCR experiments and another aliquot was further used for subculturing in a new cell culture flask containing fresh medium.

#### 4.1.3 HepG2

In the 1970s, HepG2 cells were first isolated from a patient with a hepatocellular carcinoma.<sup>77</sup>

HepG2 have an epithelial cell morphology and were cultured in *DMEM completed growth medium* in a cell culture flask. Once the cells showed 80 % confluence, they were subcultured (usually 72 h). In this process, the old medium was removed, and the cells were washed with 10 ml PBS. To detach the cells from the surface, they were treated with 3 ml trypsin/EDTA and incubated for 5-7 minutes. After incubation, 8 ml of *DMEM completed growth medium* was added and the cells were resuspended. 1 ml was taken to determine the cell number. A certain number of the cells was subcultured in a new cell culture flask with fresh medium and another desired number of cells was used for further planned qPCR experiments.

#### 4.1.4 Freezing

Depending on the cell lines, cells were passaged as described in **Methods 4.1.1 - 4.1.3**. After cell number determination, cells were centrifuged and resuspended in *freezing medium* with a concentration of  $1 \times 10^6$  cells/ml. 1 ml of the cell suspension was transferred to a cryovial and placed on ice. The cryovials were then stored at -20 °C for one hour and then placed at -80 °C for one day. After the 24 hours, the cryovials were placed in liquid nitrogen for long-term storage.

#### 4.1.5 Thawing

The cryovials were removed from the liquid nitrogen. They must be thawed almost completely in a 37 °C water bath (an ice crystal should still be visible in the center of the liquid). The cells were poured and resuspended in 10 ml of *complete growth medium*. The resuspended cells were transferred to a cell culture flask (containing another 10 ml medium) for further cultivation.

## 4.2 Luciferase reporter gene assay in HEK293 cells

Luciferase reporter gene assays are a simple and useful method to determine the activity of transcription factors and promoters. In this process, a reporter gene, which is under the control of a response element, is measured. The reporter gene, in this work the firefly luciferase, catalyzes the conversion of luciferin to oxyluciferin, emitting light. This luciferase-dependent luminescence is measured and correlates with activation of the transcription factor of interest.

Transfection of HEK293 cells with calcium phosphate, represents an efficient and cost-effective transfection method.<sup>78</sup> A major drawback of this method is its limited applicability in other cell lines and the variations in reproducibility that often occur due to factors such as incubation time and temperature.<sup>79</sup>

Bioluminescence is a widespread natural phenomenon and has been observed in organisms such as fungi, bacteria, algae, fish, firefly, and shrimp. In this phenomenon, light is produced by an enzymatic reaction, the origin of the gene used for luciferase came from the firefly, *Photinus pyralis*.<sup>80</sup>

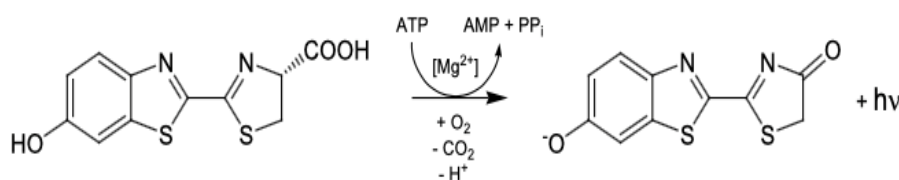


Figure 4 Luciferase catalyzes the conversion of luciferin to oxyluciferin in the presence of oxygen, ATP, and Mg<sup>2+</sup> ions, resulting in light emission that can be measured. Adapted from:

<http://www.chemgapedia.de/vsengine/glossary/de/luciferasen.glos.html> last retrieved: 14.02.2022

Using the luciferase reporter gene assay, different concentrations of flindissone were used and examined for their ability to activate the LXR $\alpha$  and/ or LXR $\beta$ .

#### 4.2.1.1 Seeding and transfection

After splitting, HEK293 were seeded at a concentration of  $6 \times 10^6$  cells in 20 ml *DMEM completed growth medium* in 15 cm Petri dishes. When the cells settled to the bottom of the Petri dish (approximately after 3 hours), the calcium phosphate transfection could begin.

Three plasmids were used for transfection: a plasmid containing the target gene for the desired nuclear receptor, in this case LXR $\alpha$  or LXR $\beta$ . A second plasmid was used encoding for the reporter gene luciferase, which is under the control of a response element. In all performed full-length receptor luciferase reporter gene assays, the ABCA1 promotor functions as the LXRE. ABCA1 contains the very typical sequence of LXRE and can therefore function as the specific response element. A third plasmid encodes for enhanced green fluorescent protein (eGFP), which serves as a control for the effectiveness of the transfection. The fluorescence generated by eGFP serves also for a normalization of the cell number in data analysis.

The reagents and plasmids of the *transfection mixture* were mixed immediately before usage ( $\text{CaCl}_2$  was added at the end). 1.5 ml of the transfection mixture were needed for each 15 cm Petri dish. A 20-minute waiting period at room temperature was performed, after which the final transfection mix was applied dropwise onto the cells. The cells were incubated overnight at 37 °C.

#### 4.2.1.2 Medium change

The next day in the morning, the old medium was removed and 20 ml fresh *DMEM completed growth medium* was added to each Petri dish.

#### 4.2.1.3 Compound treatment

Four hours later after changing the medium, cells were checked under the fluorescence microscope to confirm the efficiency of transfection. Different concentrations of the compounds (compounds were dissolved in DMSO) are diluted 1:500 with *stripped medium* (e.g., 1  $\mu\text{l}$  of the compound + 499  $\mu\text{l}$  *stripped medium*) and 100  $\mu\text{l}$  per well was placed in a 96-well plate. Each concentration was tested in quadruplicates.

#### 4.2.1.4 Reseeding

The 15 cm Petri dishes containing the transfected cells were removed from the incubator and the *DMEM completed growth medium* from the previous day was aspirated. The cells were washed with 10 ml PBS and treated with 2 ml trypsin/EDTA. When the cells were detached from the surface, trypsin was neutralized with 8 ml of *DMEM completed growth medium* and the cell suspension was transferred to a falcon tube and centrifuged at 1400 g for 8 min. The supernatant was removed, and the cell pellet was resuspended in 5 ml *stripped medium*. Using 1 ml of cell suspension, the cell number was determined in the cell counter. The cell count was used to calculate the necessary amount of cell suspension to obtain the desired concentration of  $0.5 \times 10^6$  transfected cells per 100  $\mu\text{l}$  per well. The 96-well plates were placed into the incubator.

Furthermore, a 5 cm Petri dish was seeded with a concentration of  $1 \times 10^6$  HEK293 cells in 5 ml *DMEM completed growth medium* on the same day as the transfected cells. However, these were not transfected and served as a growth control for the cells. The untransfected cells were also washed with PBS as described above and detached from the surface with trypsin/EDTA and reseeded at a concentration of  $0.5 \times 10^6$  cells per well in 200  $\mu\text{l}$ .

#### 4.2.1.5 Measurements

After an incubation period of 18 hours, the medium was aspirated, and the 96-well plate was stored at  $-80^\circ\text{C}$  for at least one hour until cell lysis.

50  $\mu\text{l}$  of *luciferase lysis buffer* was added to each well to lyse the cells. The 96-well plate was placed on the Multi-Microplate Genie™ shaker (Scientific Industries Inc.) for 10 minutes and then 40  $\mu\text{l}$  of lysate per well was removed and placed in an opaque 96-well plate. The measurement was performed using a TECAN Spark® microplate reader (Tecan Group Ltd.). The instrument injected ATP (injector A) and luciferin (injector B) directly into the wells and subsequently was first the fluorescence and then the luminescence measured. As stated at the beginning, the luminescence values were normalized to the fluorescence of eGFP to compensate cell number inequalities. Results were presented as relative luminescence units/relative fluorescence units (RLU/RFU) and normalized to 0.1 % DMSO.

**Table 12 Settings for TECAN measurement**

Measurement mode	Fluorescence
Emission wavelength	520 nm
Excitation wavelength	485 nm
Excitation Bandwidth	9 nm
Emission Bandwidth	20 nm
Gain	Optimal
Number of Flashes	25
Integration Time	1000 $\mu$ s
Lag Time	0 $\mu$ s
Settle Time	0 $\mu$ s
Z-position	20,000 $\mu$ m
Measurement mode	Luminescence
Integration time	2000 ms
Time between move and integration	50 ms
Attenuation	None
Well kinetic interval (minimal)	2020 ms
Well kinetic number	1
Injection settings	
Injector A volume	50 $\mu$ l
Injector A speed	150 $\mu$ l/sec
Injector B volume	50 $\mu$ l
Injector B speed	150 $\mu$ l/s
Injection mode	Standard

### 4.3 Mammalian one-hybrid assay: GAL4 luciferase assay

The GAL4/UAS luciferase assay is another luciferase reporter gene assay, and it was used in this work to investigate the ability of flindissone to activate LXR $\alpha$  and/or LXR $\beta$  via their LBD.

This methods part is analogous to **Method 4.2** Luciferase reporter gene assay in HEK293 cells. The only change is in the used plasmids.

In the GAL4/UAS luciferase assay, the LBD of LXR $\alpha$  or LXR $\beta$  is fused to the DBD of GAL4, a yeast-specific transcription factor. The GAL4 DBD binds to upstream activating sequences (UAS), that control the expression of a reporter gene luciferase. Transcription of luciferase is dependent on binding of a ligand to the LXR $\alpha$  or LXR $\beta$  LBD. When an agonist binds to the LXR LBD, transcription of luciferase is initiated. Luciferin is converted to oxyluciferin by luciferase, resulting in light emission, which can be measured.<sup>81</sup>

#### 4.4 Differentiation of THP-1 monocytes into THP-1 macrophages

Macrophages play a significant role in the development of atherosclerotic plaques and are therefore suitable for *in vitro* studies to gain better insight into cholesterol metabolism. In this work, differentiated THP-1 macrophages were used to determine the effect of flindissone on ABCA1 and ABCG1 protein and gene expression.

##### 4.4.1.1 Seeding and differentiation

THP-1 monocytes were cultured in *RPMI-1640 completed growth medium*. To differentiate THP-1 monocytes into THP-1 macrophages, cells were seeded in a 6-well plate at a concentration of  $0.8 \times 10^6$  cells in 4 ml *RPMI-1640 completed growth medium* per well and cells were treated with PMA 200 nM for 72 hours. The cells were checked under the microscope, to be sure if the differentiation was successful.

The now adherent THP-1 macrophages were washed once with 2 ml PBS per well and treated with 2 ml 2.5 % *FBS/serum-free DMEM with 20  $\mu$ g/ml cholesterol-water soluble* for an additional 24 hours.

After cholesterol loading, the medium was aspirated, and the cells were washed again with PBS. The cells were treated with the appropriate compound concentrations or 0.1 % DMSO as a control in 2 ml 0.1 % *BSA/serum-free DMEM* and incubated for another 24 hours.

The next day, cells were washed with ice-cold PBS and subjected to lysis, for later qPCR or western blot experiments.

## 4.5 Western blot

Western blot was first described by W. Neal Burnette in 1979. The actual western blot is a biochemical method and is used to transfer specific proteins to a membrane, which can then be detected with an immunological reaction.<sup>82</sup>

Before the proteins can be transferred to a membrane, the cells must be lysed so that the intracellular and membrane proteins become available. The protein mixture was separated in a polyacrylamide gel. The proteins, which are negatively charged by sodium dodecyl sulfate (SDS) coating, migrate along the electric field to the anode and are separated according to their size. During transfer, the separated proteins migrate from the polyacrylamide gel to a polyvinylidene fluoride (PVDF) membrane. After the transfer, the remaining free binding sites on the membrane, which would be available for non-specific protein binding, were blocked with milk powder or bovine serum albumin (BSA). The protein bands of the specific proteins were identified with primary antibodies. To remove the unbound antibodies, the membrane was washed with tris buffered saline (TBST). The sought proteins are then detected using an immunoconjugate, a secondary antibody with the reporter enzyme horseradish peroxidase (HRP) bound to the Fc region of the primary antibody. After another washing step with TBST, the *ECL solution*, which contained luminol and H<sub>2</sub>O<sub>2</sub>, was added and chemiluminescence was released by a catalytic reaction of HRP. The released chemiluminescence is directly proportional to the amount of protein and thus serves to quantify the specific protein.

In this work, the regulatory influence of flindissone, 22-R-hydroxycholesterol and GW3965 on ABCA1 was investigated by using Western blot. The experiment was performed with differentiated THP-1 macrophages.

### 4.5.1.1 Cell lysate preparation

THP-1 monocytes were seeded in *RPMI-1640 completed growth medium* at a concentration of  $0.8 \times 10^6$  cells per well and cells were differentiated into THP-1 macrophages with PMA as described above. After cholesterol loading THP-1 macrophages were treated with flindissone, GW3965 and 22-R-hydroxycholesterol, in *0.1% BSA/serum-free DMEM* for 24 hours (**Method 6.4**).

Cells were removed from the incubator, placed on ice, and washed once with 2 ml ice-cold PBS. The cells were lysed with 200 µl per well *RIPA lysis buffer* and incubated on

ice for 10 minutes. After the 10 minutes, the cells were scraped off and transferred into reaction tubes. The lysates were sonicated for 10 seconds at 100 % power (Sonopuls HD 2070; BANDELN electronic GmbH & Co. KG) and then centrifuged at 14,600 g for 20 minutes at 4 °C. The supernatant was transferred to new reaction tubes and stored at -80 °C.

#### 4.5.1.2 Protein quantification with Bradford assay

The Bradford assay is a photometric method for the quantitative determination of protein concentrations. Coomassie-Brilliant-Blue is a triphenylmethane dye and forms complexes with proteins in acid. This shifts the absorption maximum from 465 nm to 595 nm, which can then be measured.<sup>83</sup>

BSA standards were used to create a calibration straight (2.5 - 20 µg/ml). The lysates of the samples and the *RIPA lysis buffer* were diluted 1:10 with ddH<sub>2</sub>O and 5 µl of each dilution was taken and applied in triplicates on a 96-well plate. To the 5 µl of the diluted *RIPA lysis buffer*, 10 µl of the BSA dilution series, in ascending concentration, was applied. To the 5 µl of diluted lysates, 10 µl of ddH<sub>2</sub>O was added. 190 µl of Bradford reagent Roti-Quant® (1:5 dilution in ddH<sub>2</sub>O) was added to all samples and absorbance was measured at 595 nm in the microplate reader (Tecan Sunrise™; Tecan).

#### 4.5.1.3 Sodium dodecyl polyacrylamide gel electrophoresis

The protein mixture was separated by molecular weight via sodium dodecyl polyacrylamide gel electrophoresis (SDS-PAGE). First, the *resolving gel* (7.5 %) components were mixed and poured into the gel chamber of the Mini-PROTEAN™ 3 Cell System (Bio-Rad Laboratories). To prevent the gel from drying out and to obtain a smooth surface, the gel chamber was filled with isopropanol. After 45 minutes of waiting, the resolving gel was polymerized, the isopropanol was removed, the freshly prepared *stacking gel* was poured onto the resolving gel and the comb was inserted between the two glass panes of the gel chamber. After another 45 minutes, the *stacking gel* was also polymerized, and the comb could be removed.

Before the proteins could be separated, they were standardized with *3x sample buffer* and ddH<sub>2</sub>O to a uniform protein amount of 40 µg per well. The samples (40 µl) and the Precision Plus Protein™ (7 µl) were loaded into the appropriate wells and the proteins were separated at 100 V constant and 40 mA (for one gel) for approximately 120 minutes.



#### 4.5.1.4 Transfer to PVDF Membrane

The separated proteins were transferred to a PVDF (Immuno-blot™; Bio-Rad Laboratories) membrane, using a Mini-Trans-Blot® Electrophoretic Transfer Cell System (Bio-Rad Laboratories). Before transfer, the membrane must be activated in methanol for 1 minute. Transfer was performed at 100 V constantly for 90 minutes. To block the nonspecific binding sites, the membrane was shaken in 5 % BSA (BSA in 1x TBST) for 1 hour. Before immunodetection, the membrane was washed with 1x TBST for 3 x 5 minutes.

#### 4.5.1.5 Protein detection

The membrane was incubated at +4 C° overnight (can be incubated for up to 72 hours) with the primary antibody and washed with 1x TBST for 3 x 5 minutes the next day. The membrane was then incubated at room temperature for 1-2 hours with the HRP-conjugated secondary antibody. Again, the membrane was washed 3 x 5 minutes with 1x TBST and then incubated with *ECL solution* for 1 minute. Chemiluminescence was measured using the image analyzer (LAS 3000™; Fujifilm). The intensity of the bands was normalized to the housekeeping protein  $\alpha/\beta$ -tubulin on the same membrane. To detect  $\alpha/\beta$ -tubulin, the membrane must first be stripped. For this purpose, the membrane was washed 1 x 5 minutes with 1x TBST and then placed in 0.5 % NaOH for 15 minutes. After the 15 minutes, the membrane was washed again with 1x TBST for 3 x 5 minutes and then incubated again with the primary antibody overnight. The secondary antibody was added the next day and the development was analogous to the previous example.

### 4.6 RT-qPCR

The quantitative real-time polymerase chain reaction (RT-qPCR), or qPCR, is a method for amplifying specific DNA sequences. The principle is based on the well-known polymerase chain reaction (PCR) developed by Kary Mullis. The RT-qPCR is an analytical method to determine the expression level of a specific target gene.

To determine the amount of the DNA of interest, SYBR®-Green was used as a fluorescent marker in this work. This intercalates with the double-stranded DNA and emits fluorescence, which can be measured. Therefore, the quantification can be performed in

real time. In the initial phase of RT-qPCR, only a very small initial amount of double-stranded DNA is present in the samples, so the measured fluorescence is also very weak. With each amplification step, the amount of double-stranded DNA doubles and thus the measured intensity of the fluorescence also doubles.

#### 4.6.1.1 Primerdesign

Primers were designed using the primer designing tool, Primer-BLAST from NCBI. Before use, the primers had to be dissolved in RNase-free water to reach a concentration of 100  $\mu$ M. Then, 2  $\mu$ l of the forward and reverse primers were diluted in 36  $\mu$ l RNase-free water.

#### 4.6.1.2 Cell lysis and RNA isolation

Treatment of cells before lysis were identical for RT-qPCR and Western blot experiments.

THP-1 monocytes were seeded in *RPMI-1640 completed growth medium* at a concentration of  $0.8 \times 10^6$  cells per well and differentiated into THP-1 macrophages with the PMA treatment. Before lysis, THP-1 macrophages were treated with flindissone, GW3965, and 22-hydroxycholesterol in *0.1 % BSA/serum-free DMEM* for 24 hours (**Method 6.4**).

HepG2 cells were seeded at a concentration of  $0.6 \times 10^6$  cells per well in *DMEM completed growth medium*. HepG2 cells were subjected to the substance treatment every 24 hours for three consecutive days.

The following steps are identical for both cell lines. RNase-free filter tips were used in all subsequent steps.

After compound treatment, the medium of the cells was aspirated, and the cells were washed once with 2 ml PBS. The PBS was aspirated, and subsequent RNA isolation was performed according to the instructor information of the RNA Kit from innuPREP RNA Mini Kit 2.0<sup>®</sup> (Analytik Jena).

Just briefly, 400  $\mu$ l of lysis buffer was added onto the cells and the cells were then incubated on ice for 5 minutes. The lysate was applied onto the DNA removing column and centrifuged at 11,000 g for 2 minutes. The DNA column containing gDNA could be discarded and the lysate was mixed with 400  $\mu$ l of 70 % ethanol and applied to the RNA binding column and centrifuged again for 2 minutes at the same speed. Then, the RNA

column, which contains the RNA was washed twice with washing solutions. After the washing steps, the samples were centrifuged again for 3 min at 11,000 g to remove the remaining ethanol. Finally, RNA was eluted from the column with 60 µl RNase-free water and centrifuged again at 11,000 g.

The concentration of the samples was determined using NanoDrop™ 2000/2000c UV-Vis spectrophotometer (Thermo Fisher Scientific) and then the samples could be stored at -80 °C.

#### 4.6.1.3 Reverse transcription into cDNA

The cDNA synthesis was performed using the High-Capacity cDNA Reverse Transcription Kit (Applied Biosystem™). All components of the *2x RT Master Mix* were pipetted together according to the manufacturer's instructions to obtain a final volume of 10 µl per sample. Then 10 µl of the *2x RT Master Mix* was pipetted into each well of PCR stripes and 10 µl of the diluted isolated RNA (1 µg) was pipetted to it, so that a total volume of 20 µl per well prevailed. Samples were carefully vortexed and centrifuged and then placed into the thermal cycler.

**Table 13 Thermal cycling conditions for cDNA synthesis**

Step	Temperature	Time
Step 1	25 °C	10 min
Step 2	37 °C	120 min
Step 3	85 °C	5 min
Step 4	4 °C	∞

After reverse transcriptase, 30 µl RNase-free water was added to the 20 µl reaction volume to arrive at a concentration of 20 ng/µl assuming the reaction occurred with a 100 % efficiency. The 50 µl cDNA can be stored at -80 °C.

#### 4.6.1.4 Real-time quantitative PCR

A Light Cycler™ LC480 SYBR Green I Master Kit (Roche Diagnostics, Vienna, Austria) was used to quantify the amplified genes. 15 µl reaction volumes consisted of 13 µl *reaction mixture* and 2 µl cDNA were added to a 96-well plate. All samples were added as technical duplicates. The plate was centrifuged and sealed with a transparent foil.

**Table 14 RT-qPCR conditions**

Step	Temperature	Time
Pre-Incubation	95 °C	2 min
Amplification	95 °C	15 sec
	60 °C	1 min
Melting Curve	95 °C	5 sec
	55 °C	1 min
	98 °C	
Cooling	40 °C	∞

Data analysis was performed using LightCycler™ LC480 software. Melting curves were used to ensure that only one product was amplified. Quantitative PCR was analyzed according to the  $\Delta C_{dt}$  method. The expression of the target genes was normalized to the expression of a house keeping gene.

#### 4.7 Statistics

If no explicit remark is made in the course of the work, all experiments have been performed three times. The error bars in the graphs represent the standard deviation. Statistical significance was always determined with one-way ANOVA, followed by Dunnett's multiple comparison test to compare the mean of each column with the mean of the control column. All statistical analyses were performed with GraphPad Prism 6.0 software. P-values were considered as significant below an alpha of 0.05 and are designated with \* in the figures. \* $P \leq 0.05$ , \*\* $P \leq 0.01$ , \*\*\* $P \leq 0.001$ , \*\*\*\* $P \leq 0.0001$ .

## 5 Results

### 5.1 Flindissone can activate the full-length receptor LXR $\alpha$

The aim of the experiments was to find out whether different concentrations of flindissone can activate the full-length receptors LXR $\alpha$  and/or LXR $\beta$  by using luciferase reporter gene assays. To evaluate potency and efficacy of flindissone in comparison to known LXR ligands, the experiments were performed with the endogenous agonist 22-R-hydroxycholesterol and the synthetic LXR agonist GW3965, which also served as positive control.

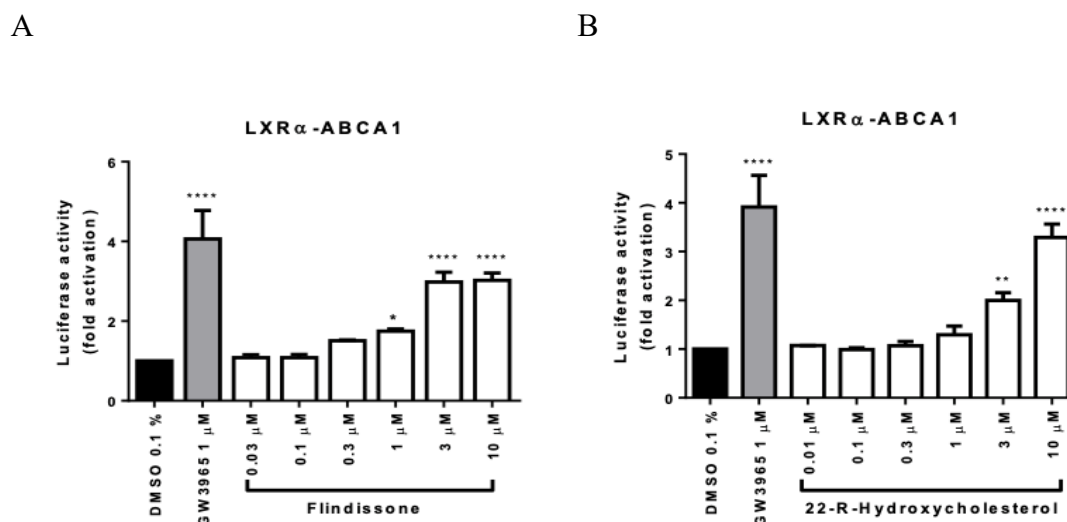


**Figure 5** Concentration dependent activation of the full-length receptor LXR $\alpha$  with A) flindissone and B) 22-R-hydroxycholesterol in the luciferase reporter gene assay. HEK293 cells were transfected using the calcium phosphate method with plasmids encoding LXR $\alpha$ , LXRE-containing luciferase reporter gene, and eGFP. Cells were treated with flindissone, GW3965 and 22-R-hydroxycholesterol at the indicated concentrations and incubated at 37 °C for 18 hours. Luminescence values were normalized to eGFP fluorescence values. Results are presented as fold activation, normalized to the solvent control DMSO. Data are shown as means  $\pm$  SD of three biological replicates, which were performed in technical quadruplicates. Statistical analysis was performed using one-way ANOVA followed by Dunnett's multiple comparison test to compare the mean of each experimental group with the mean of the control DMSO. P-values were considered as significant below an alpha of 0.05. \*P  $\leq$  0.05, \*\*P  $\leq$  0.01, \*\*\*P  $\leq$  0.001, \*\*\*\*P  $\leq$  0.0001.

**Figure 5A** shows that flindissone can significantly activate the full-length receptor LXR $\alpha$  at concentrations of 1  $\mu$ M, 3  $\mu$ M and 10  $\mu$ M. At concentrations of 30 nM and 100 nM, no

activation of LXR $\alpha$  can be observed. Flindissone concentrations between 300 nM and 10  $\mu$ M can activate LXR $\alpha$  in a dose-dependent manner. With an increase in the concentration from 3  $\mu$ M to 10  $\mu$ M, an enhancement in LXR $\alpha$  activity is no longer apparent and a plateau is reached.

22-R-hydroxycholesterol, which is structurally very similar to flindissone, can significantly activate LXR $\alpha$  at concentrations of 3  $\mu$ M and 10  $\mu$ M. At concentrations between 10 nM and 1  $\mu$ M, there is almost no activation visible. From 1  $\mu$ M onwards, 22-R-hydroxycholesterol can activate LXR $\alpha$  in a dose-dependent manner too.

If flindissone and 22-R-hydroxycholesterol are compared to each other, then the conclusion would be, that both ligands act very similar in their activation of LXR $\alpha$ . Both ligands cannot activate LXR $\alpha$  at concentrations under 1  $\mu$ M. Flindissone shows a fold induction at 1  $\mu$ M and 3  $\mu$ M of almost 2 and 3 and can therefore activate the LXR $\alpha$  more compared to 22-R-hydroxycholesterol, which shows a fold induction at 1  $\mu$ M and 3  $\mu$ M of about 1.2 and 2. At 10  $\mu$ M, both ligands show an almost identical activation of LXR $\alpha$ .

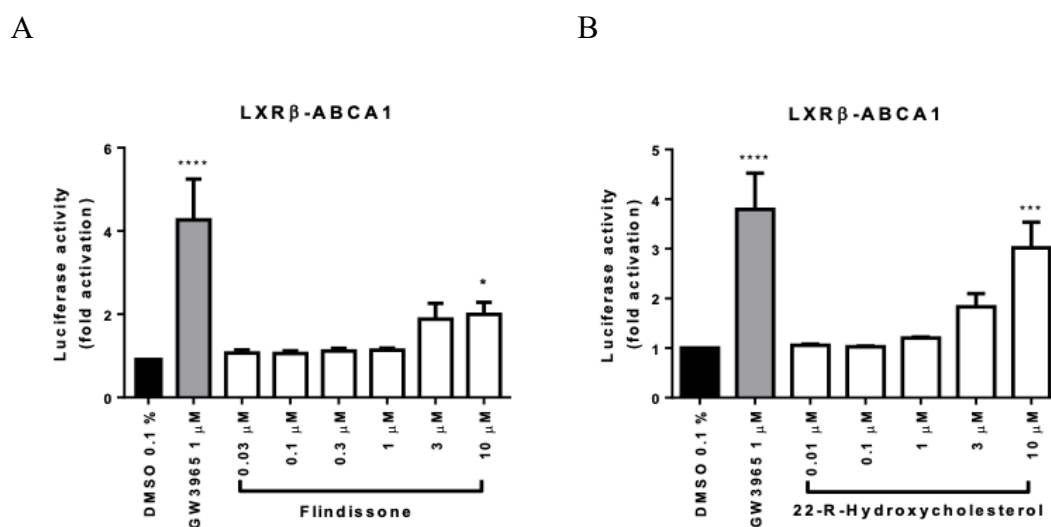


**Figure 6** Concentration dependent activation of the full-length receptor LXR $\beta$  with A) flindissone and B) 22-R-hydroxycholesterol in the luciferase reporter gene assay. HEK293 cells were transfected using the calcium phosphate method with plasmids encoding LXR $\beta$ , a LXRE-containing luciferase reporter gene, and eGFP. Cells were treated with flindissone, GW3965 and 22-R-hydroxycholesterol at the indicated concentrations and incubated at 37 °C for 18 hours. Luminescence values were normalized to eGFP fluorescence values. Results are presented as fold activation, normalized to the solvent control DMSO. Data are shown as means  $\pm$  SD of three biological replicates, which were performed in technical quadruplicates. Statistical analysis was performed using one-way ANOVA followed by Dunnett's multiple comparison test to compare the mean of each experimental group with the mean of the control DMSO. P-values were considered as significant below an alpha of 0.05. \*P  $\leq$  0.05, \*\*P  $\leq$  0.01, \*\*\*P  $\leq$  0.001, \*\*\*\*P  $\leq$  0.0001.

Flindissone can significantly activate LXR $\beta$  at a concentration of 10  $\mu$ M. A transition into a plateau sets in when the concentration is increased from 3  $\mu$ M to 10  $\mu$ M. No activation of LXR $\beta$  can be noticed at flindissone concentrations between 30 nM and 1  $\mu$ M.

22-R-hydroxycholesterol can significantly activate LXR $\beta$  with a 3-fold induction at 10  $\mu$ M. At the concentrations between 10 nM and 1  $\mu$ M, no activation of LXR $\beta$  can be observed.

Regarding the activation of LXR $\beta$ , the two ligands differ from each other. Especially, the 10  $\mu$ M of 22-R-hydroxycholesterol can activate LXR $\beta$  much more than 10  $\mu$ M flindissone.

In conclusion, according to the data of the luciferase reporter gene assays on the full-length receptors, flindissone shows some selectivity for LXR $\alpha$ .

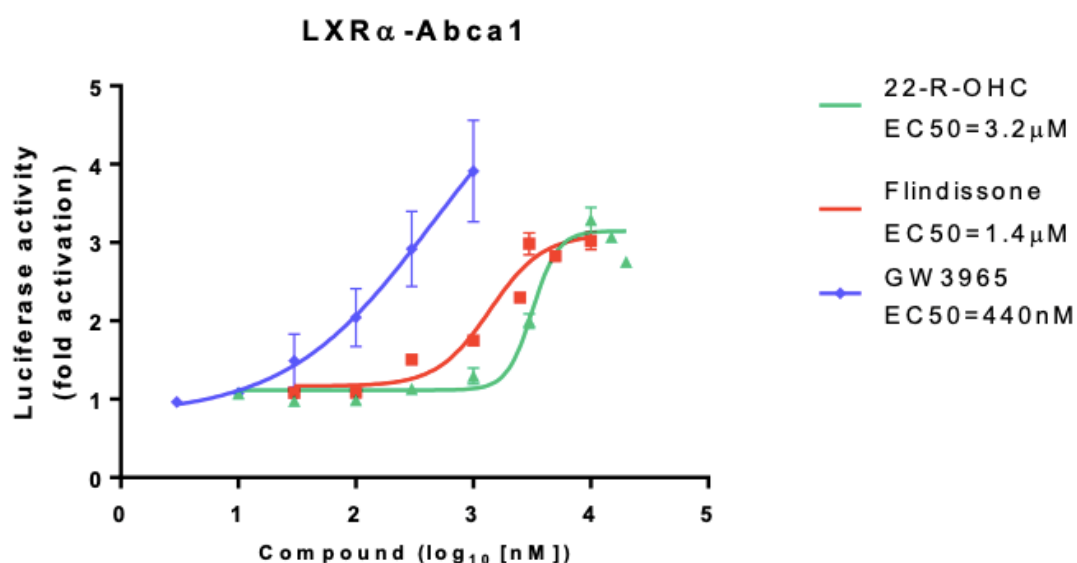


**Figure 7** Dose response curve of flindissone, GW3965 and 22-R-hydroxycholesterol on the full-length receptor LXR $\alpha$ . Results are shown as fold activation, compared to control DMSO. GW3965 represents the positive control in the experiment. Data are shown as means  $\pm$  SEM of at least three independent experiments, which were performed in quadruplicates. To calculate the EC50 values data were non-linearly transformed and curve fitted in GraphPad Prism.

When the three agonists are compared with their EC50 values (the effective concentration at which a half-maximal effect is observable) to each other, GW3965 can activate the LXR $\alpha$  with an EC50 value of 440 nM. After GW3965 comes flindissone with an EC50 of 1.4  $\mu$ M and 22-R-hydroxycholesterol with an EC50 value of 3.2  $\mu$ M.

## 5.2 Activation of LXR $\alpha$ and LXR $\beta$ via LBD

The aim of the GAL4/UAS luciferase experiments was to find out whether flindissone can activate LXR $\alpha$  and/or LXR $\beta$  via their LBD. Again, in the GAL4/UAS luciferase assays, 22-R-hydroxycholesterol was used as a comparison to flindissone and the synthetic LXR agonist GW3965 was used as the positive control.

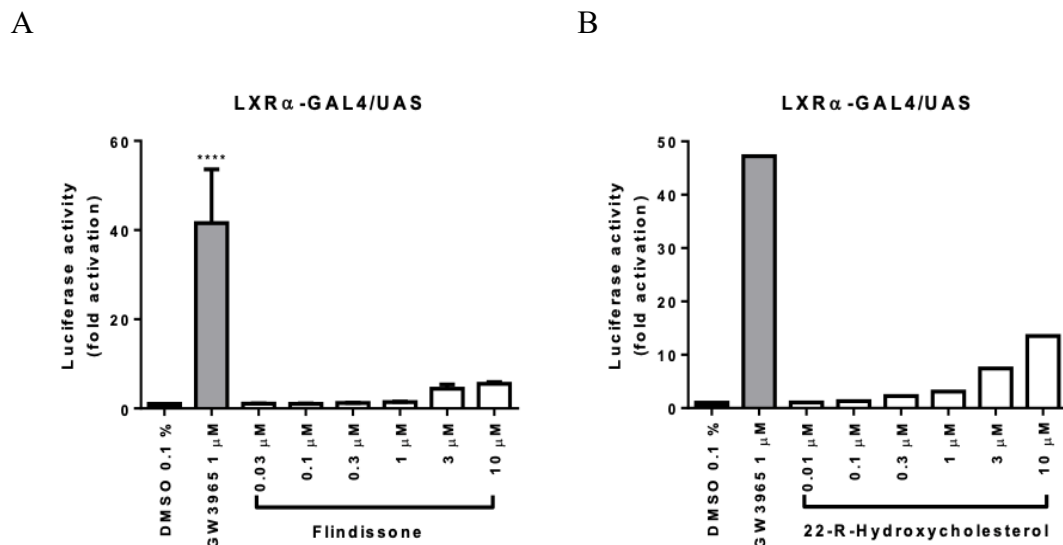


**Figure 8** Concentration dependent activation of the LXR $\alpha$  LBD with A) flindissone and B) 22-R-hydroxycholesterol in the mammalian one-hybrid GAL4/UAS luciferase assay. HEK293 cells were transfected by the calcium phosphate method using expression plasmid encoding a protein consisting of the yeast GAL4-DBD fused to the LBD of LXR $\alpha$ . The GAL4 DBD recognizes specific UAS which is fused to the luciferase reporter gene. Cells were then treated with flindissone, 22-R-hydroxycholesterol, GW3965 or DMSO (0.1%) at indicated concentrations for 18 hours, after which luminescence was measured and normalized to eGFP fluorescence. Results are shown as fold activation, compared to control DMSO (0.1%). A) Data are shown as means  $\pm$  SD of at least three independent experiments, which were performed in quadruplicates. Statistical analysis was performed using one-way ANOVA followed by Dunnett's multiple comparison test to compare the mean of each experimental group with the mean of the control DMSO. P-values were considered as significant below an alpha of 0.05. \* $P \leq 0.05$ , \*\* $P \leq 0.01$ , \*\*\* $P \leq 0.001$ , \*\*\*\* $P \leq 0.0001$ . B) Data are shown as means of one experiment, which was performed in quadruplicates. No statistical analysis was performed in the GAL4/UAS luciferase assay with the endogenous ligand 22-R-hydroxycholesterol.

**Figure 8A** shows that flindissone can only slightly activate LXR $\alpha$  via its LBD at concentrations of 3  $\mu$ M and 10  $\mu$ M and do not reach statistical significance. Concentrations between 30 nM and 1  $\mu$ M cannot activate LXR $\alpha$  via the LBD. Based on the available data, a tendency can be observed, that 22-R-hydroxycholesterol can activate LXR $\alpha$  via the LBD in a dose-dependent manner. Concentrations of 3  $\mu$ M and 10  $\mu$ M show a weak activation compared to 1  $\mu$ M GW3965.



If the two agonists are compared to each other, 22-R-hydroxycholesterol can activate LXR $\alpha$  more strongly via the LBD than flindissone, especially at a concentration of 10  $\mu$ M. Nevertheless, more data are necessary to draw a final conclusion.

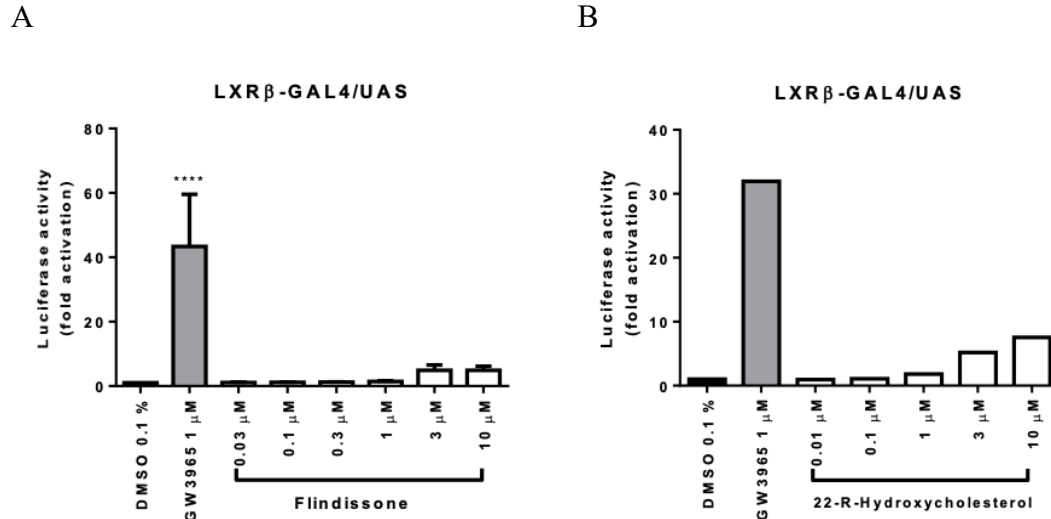


**Figure 9** Concentration dependent activation of LXR $\beta$  LBD with A) flindissone and B) 22-R-hydroxycholesterol in the mammalian one-hybrid GAL4/UAS luciferase assay. HEK293 cells were transfected by the calcium phosphate method using expression plasmid encoding a protein consisting of the yeast GAL4-DBD fused to the LBD of LXR $\beta$ . The GAL4 DBD recognizes specific UAS which is fused to the luciferase reporter gene. Cells were then treated with flindissone, 22-R-hydroxycholesterol, GW3965 or DMSO (0.1%) at indicated concentrations for 18 hours, after which luminescence was measured and normalized to eGFP fluorescence. Results are shown as fold activation, compared to control DMSO (0.1%). A) Data are shown as means  $\pm$  SD of at least three independent experiments, which were performed in quadruplicates. Statistical analysis was performed using one-way ANOVA followed by Dunnett's multiple comparison test to compare the mean of each experimental group with the mean of the control DMSO. P-values were considered as significant below an alpha of 0.05. \* $P \leq 0.05$ , \*\* $P \leq 0.01$ , \*\*\* $P \leq 0.001$ , \*\*\*\* $P \leq 0.0001$ . B) Data are shown as means of one experiment, which was performed in quadruplicates. No statistical analysis was performed in the GAL4/UAS luciferase assay with the endogenous ligand 22-R-hydroxycholesterol.

Flindissone shows a very weak activation of LXR $\beta$  via its LBD at concentrations of 3  $\mu$ M and 10  $\mu$ M and do not reach statistical significance. Concentrations between 30 nM and 1  $\mu$ M show no activation at all.

22-R-hydroxycholesterol can activate LXR $\beta$  via the LBD in a dose-dependent manner. In particular, the concentrations of 3  $\mu$ M and 10  $\mu$ M show an activation of LXR $\beta$  via the LBD, albeit only slightly. The concentrations between 10 nM and 1  $\mu$ M show almost no activation. But still, more data is needed to make a definitive statement.

If the two agonists are compared with each other, they behave in their activation of LXR $\beta$  very similarly to the LXR $\alpha$  GAL4/UAS experiments. 22-R-hydroxycholesterol can

activate the LXR $\beta$  via the LBD stronger compared to flindissone, especially at a concentration of 10  $\mu$ M. However, the experiments with 22-R-hydroxycholesterol were performed only once and for a final conclusion the experiments should be repeated.

### 5.3 Cotreatment experiments

The data from the GAL4/UAS luciferase assay in **figure 8** and **figure 9** showed that flindissone can only slightly activate LXR $\alpha$  and LXR $\beta$  via their LBD. To find out more about the binding mechanism of flindissone on LXR $\alpha$ , cotreatment experiments with flindissone plus 1  $\mu$ M GW3965, were performed.

The cotreatment was tested on the full-length receptor luciferase reporter gene assay and on the GAL4/UAS luciferase assay.

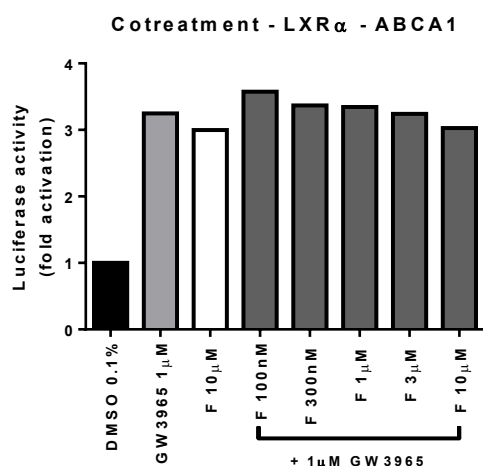


**Figure 10** Cotreatment with different flindissone concentrations plus 1  $\mu$ M GW3965 on LXR $\alpha$  in the luciferase reporter gene assay. HEK293 cells were transfected using the calcium phosphate method with expression plasmids encoding LXR $\alpha$ , LXRE-containing luciferase reporter gene, and eGFP (as internal control). Cells were treated with flindissone and GW3965 or cotreated with flindissone plus GW3965 at indicated concentrations for 18 hours, and then luminescence was measured and normalized to eGFP fluorescence. Results are presented as fold activation, normalized to the solvent control DMSO. The single compound treatments of GW3965 (1  $\mu$ M) and flindissone (10  $\mu$ M) serves as a comparison and positive control. Data are shown as means of one experiment, which was performed in quadruplicates. No statistical analysis was performed in the cotreatment experiments.

As can be seen in **figure 10**, no increased activation through the cotreatment on the full-length receptor LXR $\alpha$ , compared to the single compound treatment of either 10  $\mu$ M flindissone or 1  $\mu$ M GW3965 is visible. This shows that there is no synergism in the effect

due to the cotreatment. With increasing the flindissone concentration, there can be a slight decrease in the activation observed, which is, however, not significant. To confirm the slightly antagonistic effect, the experiments would have to be repeated.

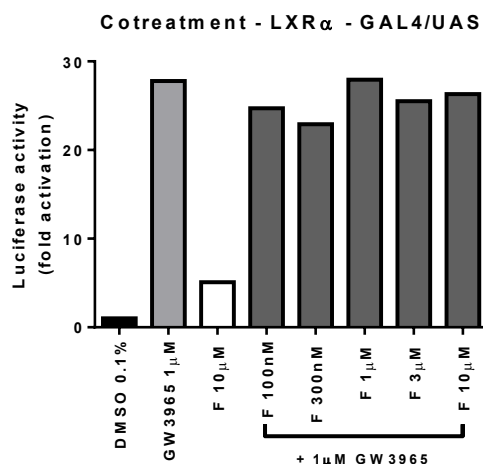


**Figure 11** Cotreatment with different flindissone concentrations plus 1  $\mu$ M GW3965 on LXR $\alpha$  in the mammalian one-hybrid assay GAL4/UAS luciferase assay. HEK293 cells were transfected by the calcium phosphate method using expression plasmid encoding a protein consisting of the yeast GAL4-DBD fused to the LBD of LXR $\alpha$ . The GAL4 DBD recognizes specific UAS which is fused to the luciferase reporter gene. Cells were treated with flindissone and GW3965 or cotreated with flindissone plus GW3965 for 18 hours, after that luminescence was measured and normalized to eGFP fluorescence. Results are shown as fold induction, compared to control DMSO. The single treatments of GW3965 and flindissone serves as a comparison and positive control. Data are shown as means of one experiment, which was performed in quadruplicates. No statistical analysis was performed in the cotreatment experiments.

According to the data in **figure 11**, no synergistic effect is apparent in the cotreatment experiments of different flindissone concentrations plus 1  $\mu$ M GW3965 in the GAL4/UAS luciferase assay. A very slight reduction of the activity in almost all cotreatments, except for 1  $\mu$ M flindissone plus 1  $\mu$ M GW3965, can be observed. In this case the activity is unchanged compared with the single compound treatment of 1  $\mu$ M GW3965. However, this exception is probably because the experiment was performed only once. Nevertheless, all results show neither significance, nor concentration-dependent inhibition.

## 5.4 Flindissone enhances ABCA1 and ABCG1 in THP-1 macrophages

To investigate the potential of flindissone to promote cholesterol efflux in macrophages, different concentrations of flindissone were tested for their ability to induce ABCA1 and ABCG1 gene and protein expression. To assess the gene expression of ABCA1 and ABCG1, RT-qPCR was performed. To confirm the results of ABCA1 gene expression at the protein level, Western blot was performed.

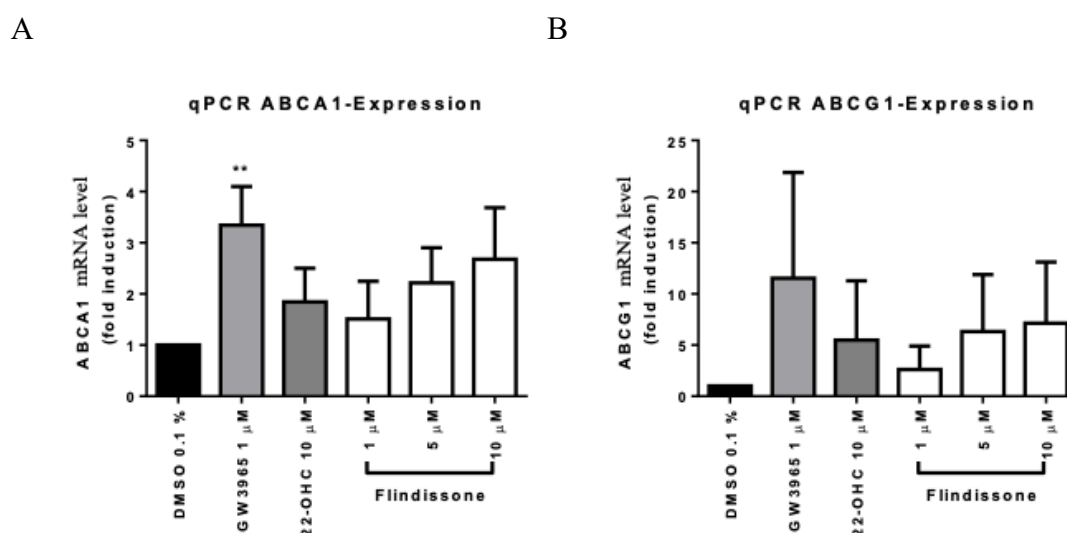


**Figure 12** Effect of different flindissone concentration on ABCA1 and ABCG1 mRNA level in THP-1 macrophages. THP-1 monocytes were treated with PMA (200 nM) for 72 h. After differentiation, THP-1 macrophages were loaded with cholesterol (20 g/ml) for 24 h and after that the cells were treated with different flindissone concentrations, GW3965 (1  $\mu$ M), 22-R-hydroxycholesterol (10  $\mu$ M) and DMSO (0.1 %) in 0.1 % BSA/serum free DMEM for another 24 h. The ABCA1 and ABCG1 mRNA level were measured by RT-qPCR. Results are shown as fold induction, compared to solvent vehicle DMSO (0.1%). GW3965 serves as the positive control and 22-R-hydroxycholesterol is used as comparison. ABCA1 gene level was normalized to the house keeping gene PPIA. Data are shown as means  $\pm$  SD of at least three independent experiments, which were performed in duplicates. Statistical significance was determined with one-way ANOVA, followed by Dunnett's multiple comparison test. \* $P \leq 0.05$ , \*\* $P \leq 0.01$ , \*\*\* $P \leq 0.001$ .

**Figure 12A** demonstrates the trend of how flindissone can induce ABCA1 gene expression in a concentration-dependent manner. 10  $\mu$ M flindissone shows a fold induction of nearly 3 and can induce ABCA1 gene expression stronger than 10  $\mu$ M 22-R-hydroxycholesterol. Due to very high standard deviations, 1  $\mu$ M GW3965 is the only representative of the three LXR agonists that can achieve significant value. 1  $\mu$ M GW3965 with a fold induction of 3.2, can increase ABCA1 mRNA level clearly more

than 1  $\mu$ M flindissone. 10  $\mu$ M flindissone and 1  $\mu$ M GW3965 show an almost equal induction of ABCA1 mRNA level.

Also, a trend of increased ABCG1 gene expression due to flindissone can be observed in **figure 12B**. The positive control GW3965 1  $\mu$ M can clearly stimulate ABCG1 expression more than all flindissone concentrations and 22-R-hydroxycholesterol. The standard deviation of the results in **figure 12B** is quite high and no statistical significance is evident. The experiment should therefore be repeated.

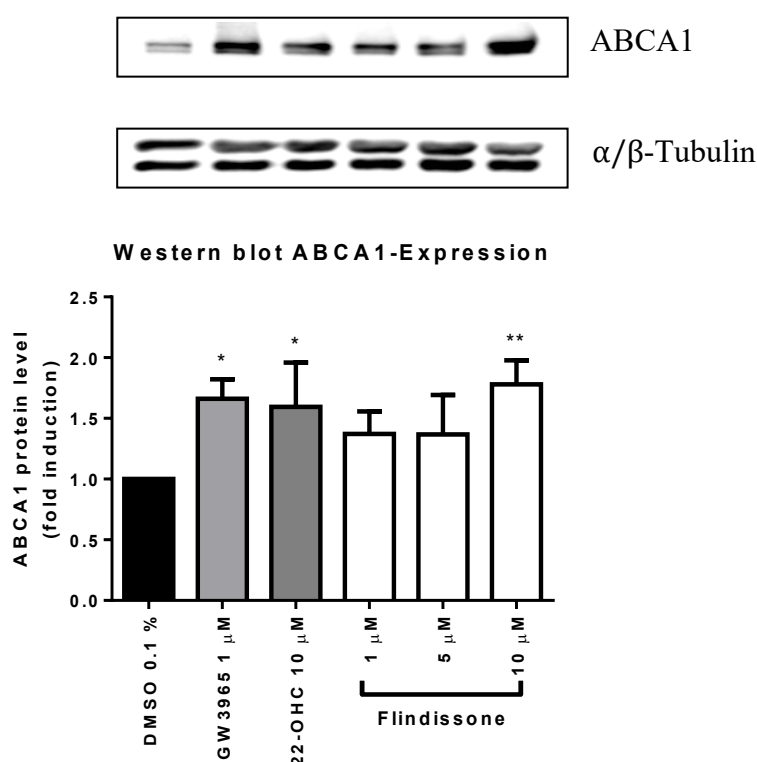


**Figure 13** Effect of different flindissone concentration on ABCA1 protein level in THP-1 macrophages. THP-1 cells were treated with PMA (200 nM) for 72 h. After differentiation, THP-1 macrophages were loaded with cholesterol (20  $\mu$ g/ml) for 24 h and after that the cells were treated with different flindissone concentrations, GW3965 (1  $\mu$ M), 22-R-hydroxycholesterol (10  $\mu$ M) and DMSO (0.1 %) in 0.1 % BSA/serum free DMEM for another 24 h. The ABCA1 protein level was determined by western blot analyses. Results are shown as fold induction, compared to solvent vehicle DMSO (0.1%). GW3965 serves as the positive control and 22-R-hydroxycholesterol is used as comparison. ABCA1 protein level was normalized to the house keeping protein  $\alpha/\beta$ -tubulin. Data are shown as means  $\pm$  SD of at least three independent experiments. Statistical significance was determined with one-way ANOVA, followed by Dunnett's multiple comparison test. \* $P \leq 0.05$ , \*\* $P \leq 0.01$ , \*\*\* $P \leq 0.001$ .

Induction of ABCA1 protein level occurs by all three agonists shown in **figure 13**. Flindissone shows a trend in the induction of ABCA1 protein level in a dose-dependent

manner. 10  $\mu$ M flindissone, 10  $\mu$ M 22-R-hydroxycholesterol and 1  $\mu$ M GW3965 show a significant level.

In conclusion, flindissone can induce ABCA1 and ABCG1 expression in a concentration-dependent manner. However, the standard deviations are often very high, especially in the RT-qPCR experiments, resulting in no significance and therefore often only a trend of induction of ABCA1 and ABCG1 gene expression can be observed.

### 5.5 The effect of flindissone on SREBP1 gene expression in HepG2 cells

Activation of LXR by the synthetic ligands GW3965 and T0901317 leads to increased expression of genes involved in *de novo* lipogenesis in the liver. This can lead to the development of hypertriglyceridemia and subsequently to hepatic steatosis.<sup>47,58</sup> As mentioned in the introduction, LXR agonists can promote gene expression of FAS, ACC, and SCD-1 in the liver via upregulating SREBP1c transcription.<sup>47</sup>

To investigate the effect on SREBP1c gene expression in the liver, HepG2 cells were treated with the compounds for three consecutive days and gene expression of the corresponding target genes was determined by RT-qPCR.

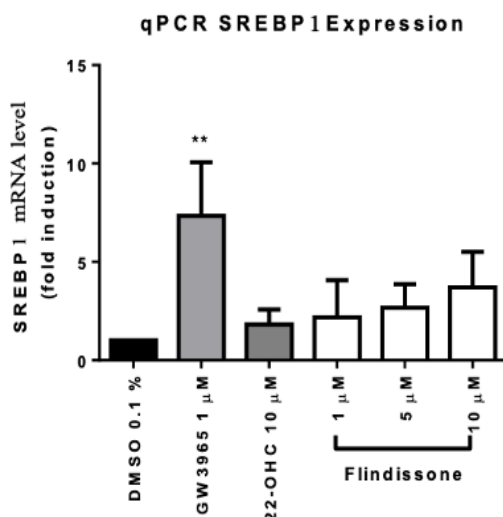


**Figure 14** The effect of different flindissone concentrations on SREBP1 mRNA level in HepG2 cells. For three days, HepG2 cells were treated every 24 h with the indicated concentrations of flindissone, GW3965, 22-R-hydroxycholesterol and DMSO. SREBP1 mRNA level was determined by RT-qPCR. Results are shown as fold induction, compared to solvent vehicle DMSO. SREBP1 gene level was normalized to housekeeping gene GAPDH. Statistical analysis was performed using one-way ANOVA followed by Dunnett's multiple comparison test to compare the mean of each experimental group with the mean of the control DMSO. P-values were considered as significant below an alpha of 0.05. \* $P \leq 0.05$ , \*\* $P \leq 0.01$ , \*\*\* $P \leq 0.001$ , \*\*\*\* $P \leq 0.0001$ .

As expected, the synthetic ligand GW3965 strongly induces SREBP1 gene expression in HepG2 cells. 1  $\mu$ M GW3965 achieves a significant value with an approximate 7-fold fold induction. All flindissone concentrations show a tendency to induce SREBP1 gene expression only very slightly. The highest tested flindissone concentration (10  $\mu$ M) activates SREBP1 only half as much as 1  $\mu$ M GW3965. Interestingly, the endogenous ligand 22-R-hydroxycholesterol exhibits very low SREBP1 activation.

## 5.6 The effect of flindissone on the LDLR gene expression in HepG2 cells

The LDLR represents on the one hand an indirect and on the other hand a direct LXR target gene. The activation of LXR can increase the IDOL expression. IDOL is an E3 ubiquitin protein ligase that can ubiquitylate and degrade the LDLR, resulting in less LDL being absorbed via the LDLR in the liver.<sup>45</sup> Interestingly, activation of LXR $\alpha$  can directly promote expression of LDLR and thereby lowering plasma cholesterol levels by increasing uptake of LDL.<sup>46</sup>

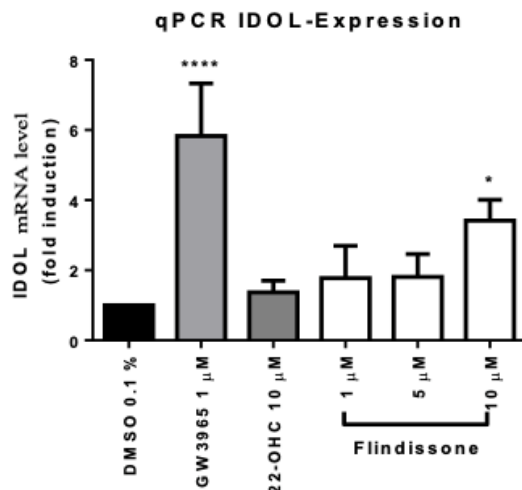


**Figure 15** The effect of different flindissone concentrations on IDOL mRNA level in HepG2 cells. For three days, HepG2 cells were treated every 24 h with the indicated concentrations of flindissone, GW3965, 22-R-hydroxycholesterol and DMSO. IDOL mRNA level was determined by RT-qPCR. Results are shown as fold induction, compared to solvent vehicle DMSO. IDOL gene level was normalized to housekeeping gene GAPDH. Statistical analysis was performed using one-way ANOVA followed by Dunnett's multiple comparison test to compare the mean of each experimental group with the mean of the control DMSO. P-values were considered as significant below an alpha of 0.05. \*P  $\leq$  0.05, \*\*P  $\leq$  0.01, \*\*\*P  $\leq$  0.001, \*\*\*\*P  $\leq$  0.0001.

10  $\mu$ M flindissone significantly increases IDOL gene expression. 1  $\mu$ M and 5  $\mu$ M flindissone enhances IDOL gene expression very weakly with a 1.9-fold induction and do not reach significance. The synthetic LXR agonist GW3965 shows a very strong increasement of IDOL gene expression. 10  $\mu$ M 22-R-hydroxycholesterol shows almost no induction of IDOL gene expression.

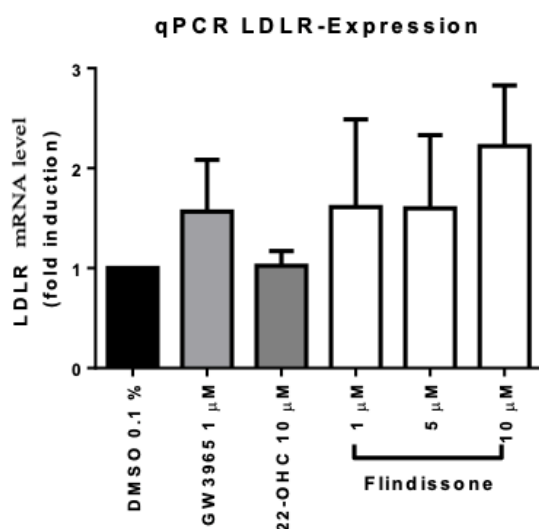


**Figure 16** The effect of different flindissone concentrations on LDLR mRNA level in HepG2 cells. For three days, HepG2 cells were treated every 24 h with the indicated concentrations of flindissone, GW3965, 22-R-hydroxycholesterol and DMSO. LDLR mRNA level was determined by RT-qPCR. Results are shown as fold induction, compared to solvent vehicle DMSO. LDLR gene level was normalized to housekeeping gene GAPDH. Statistical analysis was performed using one-way ANOVA followed by Dunnett's multiple comparison test to compare the mean of each experimental group with the mean of the control DMSO. P-values were considered as significant below an alpha of 0.05. \* $P \leq 0.05$ , \*\* $P \leq 0.01$ , \*\*\* $P \leq 0.001$ , \*\*\*\* $P \leq 0.0001$ .

**Figure 16** shows that a tendency for induction of LDLR gene expression is evident with all flindissone concentrations. Interestingly, 1  $\mu$ M GW3965 induces LDLR gene expression not so strongly as expected. It increases the LDLR expression to the same extent as 1  $\mu$ M flindissone. 22-R-hydroxycholesterol has no effect at all on LDLR gene expression. However, in no case statistical significance was reached due to high standard deviations.



## 6 Discussion

LXR is a master regulator in cholesterol metabolism and therefore serves as a potential therapeutic target in combating ASCVD. The search for suitable ligands that can activate the LXR receptor in a gene- or tissue-selective manner could represent an approach for a novel therapy for the treatment of atherosclerosis.

The main goal of this work was to test whether and how strongly flindissone can activate the LXR $\alpha$  and/or LXR $\beta$  and to find out how this activation affects the expression of LXR target genes. The structure of flindissone was first clarified by Liang et al. in 1989 and flindissone is mentioned several times in the literature because of its antiproliferative and antibacterial properties.<sup>69,71,74</sup>

By using luciferase reporter gene assays, it has been found that flindissone can relatively selectively activate the full-length receptor LXR $\alpha$  in a dose-dependent manner (**Figure 5**). Flindissone shows an EC<sub>50</sub> value of 1.4  $\mu$ M and can thereby induce the activity of LXR $\alpha$  more potent than the endogenous ligand 22-R-hydroxycholesterol (EC<sub>50</sub>=3.2  $\mu$ M). The synthetic ligand GW3965, with an EC<sub>50</sub> value of 440 nM, can activate the LXR $\alpha$  3.11 times stronger than flindissone (**Figure 7**). Perhaps, due to its poor solubility, flindissone cannot significantly activate the LXR $\alpha$  in the nanomolar range, but only at a concentration greater than or equal to 1  $\mu$ M.

The low solubility of flindissone may also provide an explanation why flindissone can only very slightly activate LXR $\alpha$  and LXR $\beta$  via the LBD in the GAL4/UAS luciferase assay (**Figure 8** and **Figure 9**).

The data from the cotreatment experiments are not sufficient to make a definite statement about a slightly antagonistic effect of flindissone on the LBD of LXR $\alpha$  in the GAL4/UAS luciferase assay. The experiments should be repeated in the future to draw a reliable conclusion. (**Figure 10** and **Figure 11**).

Data from this work demonstrated a clear trend, that flindissone can upregulate the expression of the ABC transporters, ABCA1 and ABCG1 in THP-1 macrophages. After flindissone treatment ABCA1 level was increased in a dose-dependent manner in Western blot and RT-qPCR experiments (**Figure 12A** and **Figure 13**). In the upregulation of the cholesterol efflux transporter ABCG1 by flindissone, a trend of concentration-dependent activation was observed in RT-qPCR experiments (**Figure 12B**).

It is well known that the synthetic ligand GW3965 promotes SREBP1c expression in the liver, which results in the induction of genes involved in *de novo* lipogenesis. This could be also confirmed in this work. The hope was that flindissone would represent a novel LXR ligand that would not or would just very slightly promote SREBP1 gene expression. By treating HepG2 cells with 1  $\mu$ M GW3965, an 8-fold induction of SREBP1 mRNA level was observed. In comparison, 1  $\mu$ M flindissone achieved a 2.5-fold induction of SREBP1 mRNA level. 10  $\mu$ M flindissone increases SREBP1 gene expression with a 4-fold induction only half as much compared with 1  $\mu$ M of the synthetic ligand. Interestingly, 10  $\mu$ M 22-R-hydroxycholesterol increases SREBP1 gene expression just very slightly (**Figure 14**).

As mentioned in the introduction, the E3 ubiquitin ligase IDOL represents an LXR target gene. LXR agonists can promote the degradation of LDLR via an indirect mechanism by inducing the transcription of IDOL. Resulting, less LDL is taken up by the liver and plasma cholesterol levels increase.<sup>45</sup> It has been reported in the literature that the inhibition of IDOL could be a potential therapeutic target in atherosclerosis treatment.<sup>84</sup> This work once again confirms that IDOL is an LXR target gene. 1  $\mu$ M GW3965 exhibits a 5.9-fold induction of IDOL mRNA level in HepG2 cells. In comparison, 1  $\mu$ M flindissone activates the IDOL mRNA level with a 1.9-fold induction. Only 10  $\mu$ M flindissone achieves a significant value of IDOL mRNA level (3.1-fold induction). In summary, GW3965 promotes the induction of IDOL expression even at very low concentrations, whereas flindissone shows almost no enhancement of IDOL expression at concentrations up to 5  $\mu$ M (**Figure 15**).

With the approval of the monoclonal antibodies alirocumab and evolocumab, which belong to the group of PCSK9 inhibitors, the LDLR has gained great interest as a therapeutic target in the treatment of atherosclerosis.<sup>85</sup> LDLR is a direct target of LXR. LXR agonists, can increase the expression of LDLR (via SREBP2 independent pathway) and consequently through the uptake of LDL in the liver, LDL cholesterol level in plasma would decrease.<sup>46</sup> 1  $\mu$ M GW3965 and 1  $\mu$ M flindissone show with a 1.5-fold induction an equal enhancement of LDLR mRNA (also 5  $\mu$ M flindissone). 10  $\mu$ M flindissone can increase LDLR mRNA level with a 2.2-fold fold induction (**Figure 16**). These results indicate that flindissone tends to increase gene expression of LDL.

Interestingly, 10  $\mu$ M of the endogenous ligand 22-R-hydroxycholesterol has almost no effect on IDOL and LDLR gene expression (**Figure 15** and **Figure 16**).

In summary, in this work, RT-qPCR results often have a large standard deviation, and no significant values were obtained. Therefore, often only a tendency of the resulting effect can be assumed. For clearer results with a lower standard deviation, the experiments should be repeated in anyway.

When it comes to the finding of new ligands for NR, the goal is usually to achieve an EC50 value in the nanomolar range. With an EC50 value of 1.4  $\mu$ M, flindissone is a moderately potent LXR agonist. Furthermore, flindissone should be tested for its solubility using analytical methods such as HPLC. To show the effect of flindissone on post-transcriptional regulation of SREBP1 in HepG2 cells, Western blots should be performed in the future. In general, LXR research should focus more on how the recruitment of coactivators and corepressors occurs in different tissues, to be able to search more specifically for selective tissue or gene modulators.

In summary, this work has shown that flindissone is a novel LXR $\alpha$  ligand that shows a tendency to upregulate the two ABC transporters ABCA1 and ABCG1 and could perhaps promote cholesterol efflux and thereby counteract plaque development. According to the data of the RT-qPCR experiments, flindissone increases the expression of SREBP1 in HepG2 cells significantly less than the synthetic ligand GW3965 and therefore the risk for the development of hypertriglyceridemia could possibly be reduced.

LXR would represent an excellent target for the treatment of atherosclerosis and the search for new potent but gene and tissue selective ligands should not stand still in the future.

## 7 Appendix

### 7.1 Abbreviation

#### **A**

ACC	Acetyl-CoA-carboxylase
ABCA1	ATP-binding cassette subfamily A member 1
ABCG1	ATP-binding cassette subfamily G member 1
ABCG5	ATP-binding cassette subfamily G member 5
ABCG8	ATP-binding cassette subfamily G member 8
AF	Activation function
ApoB	Apolipoprotein B
ASCVD	Atherosclerotic cardiovascular disease
ATP	Adenosine triphosphate

#### **B**

BSA	Bovine serum albumin
-----	----------------------

#### **C**

CYP7A1	Cytochrome P450 7A1
--------	---------------------

#### **D**

DBD	DNA-binding domain
ddH <sub>2</sub> O	Double distilled water
DMEM	Dulbecco's Modified Eagle's Medium
DTT	Dithiothreitol

#### **E**

eGFP	Enhanced green fluorescent protein
------	------------------------------------

**F**

FAS	Fatty acid synthase
FBS	Fetal bone serum
FH	Familial hypercholesterolaemia

**G**

GAPDH	Glycerinaldehyde 3-phosphate dehydrogenase
-------	--

**H**

HAT	Histone acetyltransferase
HDAC	Histone deacetylase
HDL	High density lipoprotein
HEK293	Human embryonic kidney 293
HMG-CoA	3-Hydroxy-3-methylglutaryl-CoA reductase
HRP	Horseradish peroxidase
HTS	High throughput screening
H12	Helix 12

**I**

IDL	Intermediate-density lipoprotein
-----	----------------------------------

**L**

LBD	Ligand-binding domain
LBP	Ligand-binding pocket
LCAT	Lecithin-cholesterol acyltransferase
LDL	Low density lipoprotein
LDL-C	Low density lipoprotein-cholesterol
LDLR	Low density lipoprotein receptor
Lp(a)	Lipoprotein a
LXR	Liver X receptor
LXRE	LXR response element

**M**

MYLIP      Myosin regulatory light chain interacting protein

**N**

NCoR      nuclear receptor co-repressor

NPC1L1      NPC1 like intracellular cholesterol transporter 1

NR      Nuclear receptor

**O**

OxLDL      Oxidized LDL

**P**

PBS      Phosphate buffered saline

PCR      Polymerase chain reaction

PCSK9      Proprotein convertase subtilisin/kexin type 9

PPIA      Peptidylpropyl isomerase A

PMA      Phorbol 12-myristate 13-acetate

PVDF      Polyvinylidene fluoride

**R**

RCT      Reverse cholesterol transport

RE      Response element

RFU      Relative fluorescence units

RIPA      Radioimmunoprecipitation assay buffer

RLU      Relative luminescence units

RPMI      Roswell Park Memorial Insitute

RT-qPCR      Quantitative real-time polymerase chain reaction

RXR      Retinoid X receptor

## S

SCAP	Sterol regulatory element-binding protein cleavage-activating protein
SCD1	Stearyl-CoA desaturase-1
SDS	Sodium dodecyl sulfate
SDS-PAGE	Sodium dodecyl polyacrylamide gel electrophoresis (SDS-PAGE)
SMC	Smooth muscle cells
SMRT	Silencing mediator of retinoic acid and thyroid hormone receptor
SR	Scavenger receptor
SRE	Steroid response element
SREBP	Sterol regulatory element-binding protein

## T

TBST	Tris buffered saline
------	----------------------

## V

VCAM	Vascular cell adhesion molecule
VLDL	Very low density lipoprotein

## 7.2 Figures

**Figure 1** Most NR consist of six functional domains: the N-terminal ligand-independent activation function-1 (AF-1), the highly conserved DNA-binding domain (DBD), between the DBD and ligand-binding domain (LBD) is the hinge domain located, the ligand-dependent activation function-2 (AF2) and the highly variable F domain located at the C-terminal end. Adopted and modified from: Mangelsdorf et al., 1995<sup>1</sup>. Created with BioRender.com ..... 5

**Figure 2 Transcriptional induction of LXR.** In the absence of a ligand, the transcription of the target genes is repressed by corepressors, such as silencing mediator of retinoic acid and thyroid hormone receptor (SMRT) or nuclear receptor co-repressor (NCoR). If the LXR/RXR heterodimer is now activated with a ligand, this causes a conformational change of the receptor: the corepressor is released, and a coactivator is recruited. Created with BioRender.com ..... 6

<b>Figure 3 Cyclization of the 17<math>\beta</math>-furan ring.</b> Adopted and modified from: Q. Tan and X. Luo 2011 <sup>67</sup> .....	13
<b>Figure 4 Luciferase catalyzes the conversion of luciferin to oxyluciferin in the presence of oxygen, ATP, and Mg<sup>2+</sup> ions, resulting in light emission that can be measured.</b> Adapted from: <a href="http://www.chemgapedia.de/vsengine/glossary/de/luciferasen.glos.html">http://www.chemgapedia.de/vsengine/glossary/de/luciferasen.glos.html</a> last retrieved: 14.02.2022 .....	28
<b>Figure 5 Concentration dependent activation of the full-length receptor LXR<math>\alpha</math> with A) flindissone and B) 22-R-hydroxycholesterol in the luciferase reporter gene assay.</b> HEK293 cells were transfected using the calcium phosphate method with plasmids encoding LXR $\alpha$ , LXRE-containing luciferase reporter gene, and eGFP. Cells were treated with flindissone, GW3965 and 22-R-hydroxycholesterol at the indicated concentrations and incubated at 37 °C for 18 hours. Luminescence values were normalized to eGFP fluorescence values. Results are presented as fold activation, normalized to the solvent control DMSO. Data are shown as means $\pm$ SD of three biological replicates, which were performed in technical quadruplicates. Statistical analysis was performed using one-way ANOVA followed by Dunnett's multiple comparison test to compare the mean of each experimental group with the mean of the control DMSO. P-values were considered as significant below an alpha of 0.05. *P $\leq$ 0.05, **P $\leq$ 0.01, ***P $\leq$ 0.001, ****P $\leq$ 0.0001. ....	39
<b>Figure 6 Concentration dependent activation of the full-length receptor LXR<math>\beta</math> with A) flindissone and B) 22-R-hydroxycholesterol in the luciferase reporter gene assay.</b> HEK293 cells were transfected using the calcium phosphate method with plasmids encoding LXR $\beta$ , a LXRE-containing luciferase reporter gene, and eGFP. Cells were treated with flindissone, GW3965 and 22-R-hydroxycholesterol at the indicated concentrations and incubated at 37 °C for 18 hours. Luminescence values were normalized to eGFP fluorescence values. Results are presented as fold activation, normalized to the solvent control DMSO. Data are shown as means $\pm$ SD of three biological replicates, which were performed in technical quadruplicates. Statistical analysis was performed using one-way ANOVA followed by Dunnett's multiple comparison test to compare the mean of each experimental group with the mean of the control DMSO. P-values were considered as significant below an alpha of 0.05. *P $\leq$ 0.05, **P $\leq$ 0.01, ***P $\leq$ 0.001, ****P $\leq$ 0.0001. ....	40



**Figure 7 Dose response curve of flindissone, GW3965 and 22-R-hydroxycholesterol on the full-length receptor LXR $\alpha$ .** Results are shown as fold activation, compared to control DMSO. GW3965 represents the positive control in the experiment. Data are shown as means  $\pm$  SEM of at least three independent experiments, which were performed in quadruplicates. To calculate the EC50 values data were non-linearly transformed and curve fitted in GraphPad Prism..... 41

**Figure 8 Concentration dependent activation of the LXR $\alpha$  LBD with A) flindissone and B) 22-R-hydroxycholesterol in the mammalian one-hybrid GAL4/UAS luciferase assay.** HEK293 cells were transfected by the calcium phosphate method using expression plasmid encoding a protein consisting of the yeast GAL4-DBD fused to the LBD of LXR $\alpha$ . The GAL4 DBD recognizes specific UAS which is fused to the luciferase reporter gene. Cells were then treated with flindissone, 22-R-hydroxycholesterol, GW3965 or DMSO (0.1%) at indicated concentrations for 18 hours, after which luminescence was measured and normalized to eGFP fluorescence. Results are shown as fold activation, compared to control DMSO (0.1%). A) Data are shown as means  $\pm$  SD of at least three independent experiments, which were performed in quadruplicates. Statistical analysis was performed using one-way ANOVA followed by Dunnett's multiple comparison test to compare the mean of each experimental group with the mean of the control DMSO. P-values were considered as significant below an alpha of 0.05. \*P  $\leq$  0.05, \*\*P  $\leq$  0.01, \*\*\*P  $\leq$  0.001, \*\*\*\*P  $\leq$  0.0001. B) Data are shown as means of one experiment, which was performed in quadruplicates. No statistical analysis was performed in the GAL4/UAS luciferase assay with the endogenous ligand 22-R-hydroxycholesterol..... 42

**Figure 9 Concentration dependent activation of LXR $\beta$  LBD with A) flindissone and B) 22-R-hydroxycholesterol in the mammalian one-hybrid GAL4/UAS luciferase assay.** HEK293 cells were transfected by the calcium phosphate method using expression plasmid encoding a protein consisting of the yeast GAL4-DBD fused to the LBD of LXR $\beta$ . The GAL4 DBD recognizes specific UAS which is fused to the luciferase reporter gene. Cells were then treated with flindissone, 22-R-hydroxycholesterol, GW3965 or DMSO (0.1%) at indicated concentrations for 18 hours, after which luminescence was measured and normalized to eGFP fluorescence. Results are shown as fold activation, compared to control DMSO (0.1%). A) Data are shown as means  $\pm$  SD of at least three independent experiments, which were performed in quadruplicates. Statistical analysis was performed using one-way ANOVA followed by Dunnett's multiple comparison test

to compare the mean of each experimental group with the mean of the control DMSO. P-values were considered as significant below an alpha of 0.05. \* $P \leq 0.05$ , \*\* $P \leq 0.01$ , \*\*\* $P \leq 0.001$ , \*\*\*\* $P \leq 0.0001$ . B) Data are shown as means of one experiment, which was performed in quadruplicates. No statistical analysis was performed in the GAL4/UAS luciferase assay with the endogenous ligand 22-R-hydroxycholesterol. .... 43

**Figure 10 Cotreatment with different flindissone concentrations plus 1  $\mu$ M GW3965 on LXR $\alpha$  in the luciferase reporter gene assay.** HEK293 cells were transfected using the calcium phosphate method with expression plasmids encoding LXR $\alpha$ , LXRE-containing luciferase reporter gene, and eGFP (as internal control). Cells were treated with flindissone and GW3965 or cotreated with flindissone plus GW3965 at indicated concentrations for 18 hours, and then luminescence was measured and normalized to eGFP fluorescence. Results are presented as fold activation, normalized to the solvent control DMSO. The single compound treatments of GW3965 (1  $\mu$ M) and flindissone (10  $\mu$ M) serves as a comparison and positive control. Data are shown as means of one experiment, which was performed in quadruplicates. No statistical analysis was performed in the cotreatment experiments. .... 44

**Figure 11 Cotreatment with different flindissone concentrations plus 1  $\mu$ M GW3965 on LXR $\alpha$  in the mammalian one-hybrid assay GAL4/UAS luciferase assay.** HEK293 cells were transfected by the calcium phosphate method using expression plasmid encoding a protein consisting of the yeast GAL4-DBD fused to the LBD of LXR $\alpha$ . The GAL4 DBD recognizes specific UAS which is fused to the luciferase reporter gene. Cells were treated with flindissone and GW3965 or cotreated with flindissone plus GW3965 for 18 hours, after that luminescence was measured and normalized to eGFP fluorescence. Results are shown as fold induction, compared to control DMSO. The single treatments of GW3965 and flindissone serves as a comparison and positive control. Data are shown as means of one experiment, which was performed in quadruplicates. No statistical analysis was performed in the cotreatment experiments. .... 45

**Figure 12 Effect of different flindissone concentration on ABCA1 and ABCG1 mRNA level in THP-1 macrophages.** THP-1 monocytes were treated with PMA (200 nM) for 72 h. After differentiation, THP-1 macrophages were loaded with cholesterol (20 g/ml) for 24 h and after that the cells were treated with different flindissone concentrations, GW3965 (1  $\mu$ M), 22-R-hydroxycholesterol (10  $\mu$ M) and DMSO (0.1 %) in 0.1 % BSA/serum free DMEM for another 24 h. The ABCA1 and ABCG1 mRNA

level were measured by RT-qPCR. Results are shown as fold induction, compared to solvent vehicle DMSO (0.1%). GW3965 serves as the positive control and 22-R-hydroxycholesterol is used as comparison. ABCA1 gene level was normalized to the house keeping gene PPIA. Data are shown as means  $\pm$  SD of at least three independent experiments, which were performed in duplicates. Statistical significance was determined with one-way ANOVA, followed by Dunnett's multiple comparison test. \* $P \leq 0.05$ , \*\* $P \leq 0.01$ , \*\*\* $P \leq 0.001$ . ..... 46

**Figure 13 Effect of different flindissone concentration on ABCA1 protein level in THP-1 macrophages.** THP-1 cells were treated with PMA (200 nM) for 72 h. After differentiation, THP-1 macrophages were loaded with cholesterol (20  $\mu$ g/ml) for 24 h and after that the cells were treated with different flindissone concentrations, GW3965 (1  $\mu$ M), 22-R-hydroxycholesterol (10  $\mu$ M) and DMSO (0.1 %) in 0.1 % BSA/serum free DMEM for another 24 h. The ABCA1 protein level was determined by western blot analyses. Results are shown as fold induction, compared to solvent vehicle DMSO (0.1%). GW3965 serves as the positive control and 22-R-hydroxycholesterol is used as comparison. ABCA1 protein level was normalized to the house keeping protein  $\alpha/\beta$ -tubulin. Data are shown as means  $\pm$  SD of at least three independent experiments. Statistical significance was determined with one-way ANOVA, followed by Dunnett's multiple comparison test. \* $P \leq 0.05$ , \*\* $P \leq 0.01$ , \*\*\* $P \leq 0.001$ . ..... 47

**Figure 14 The effect of different flindissone concentrations on SREBP1 mRNA level in HepG2 cells.** For three days, HepG2 cells were treated every 24 h with the indicated concentrations of flindissone, GW3965, 22-R-hydroxycholesterol and DMSO. SREBP1 mRNA level was determined by RT-qPCR. Results are shown as fold induction, compared to solvent vehicle DMSO. SREBP1 gene level was normalized to housekeeping gene GAPDH. Statistical analysis was performed using one-way ANOVA followed by Dunnett's multiple comparison test to compare the mean of each experimental group with the mean of the control DMSO. P-values were considered as significant below an alpha of 0.05. \* $P \leq 0.05$ , \*\* $P \leq 0.01$ , \*\*\* $P \leq 0.001$ , \*\*\*\* $P \leq 0.0001$ . ..... 48

**Figure 15 The effect of different flindissone concentrations on IDOL mRNA level in HepG2 cells.** For three days, HepG2 cells were treated every 24 h with the indicated concentrations of flindissone, GW3965, 22-R-hydroxycholesterol and DMSO. IDOL mRNA level was determined by RT-qPCR. Results are shown as fold induction, compared to solvent vehicle DMSO. IDOL gene level was normalized to housekeeping gene GAPDH. Statistical analysis was performed using one-way ANOVA followed by

Dunnett's multiple comparison test to compare the mean of each experimental group with the mean of the control DMSO. P-values were considered as significant below an alpha of 0.05. \* $P \leq 0.05$ , \*\* $P \leq 0.01$ , \*\*\* $P \leq 0.001$ , \*\*\*\* $P \leq 0.0001$ . ..... 49

**Figure 16 The effect of different flindissone concentrations on LDLR mRNA level in HepG2 cells.** For three days, HepG2 cells were treated every 24 h with the indicated concentrations of flindissone, GW3965, 22-R-hydroxycholesterol and DMSO. LDLR mRNA level was determined by RT-qPCR. Results are shown as fold induction, compared to solvent vehicle DMSO. LDLR gene level was normalized to housekeeping gene GAPDH. Statistical analysis was performed using one-way ANOVA followed by Dunnett's multiple comparison test to compare the mean of each experimental group with the mean of the control DMSO. P-values were considered as significant below an alpha of 0.05. \* $P \leq 0.05$ , \*\* $P \leq 0.01$ , \*\*\* $P \leq 0.001$ , \*\*\*\* $P \leq 0.0001$ . ..... 50

### 7.3 Tables

<b>Table 1 Structure of LXR agonists.....</b>	<b>14</b>
<b>Table 2 Supplier information.....</b>	<b>17</b>
<b>Table 3 Compounds supplier information.....</b>	<b>18</b>
<b>Table 4 Cell culture media and supplements .....</b>	<b>18</b>
<b>Table 5 Supplier information of used cell lines .....</b>	<b>20</b>
<b>Table 6 Reagents, plasmids and buffers used in the luciferase reporter gene assay .....</b>	<b>20</b>
<b>Table 7 Used plasmids in the GAL4/UAS luciferase assay .....</b>	<b>22</b>
<b>Table 8 buffers and reagents used in the Western blot experiments .....</b>	<b>22</b>
<b>Table 9 Supplier information of used antibody .....</b>	<b>24</b>
<b>Table 10 Used primers in the qPCR experiments.....</b>	<b>25</b>
<b>Table 11 Reagents used in the qPCR experiments .....</b>	<b>25</b>
<b>Table 12 Settings for TECAN measurement.....</b>	<b>31</b>
<b>Table 13 Thermal cycling conditions for cDNA synthesis .....</b>	<b>37</b>
<b>Table 14 RT-qPCR conditions.....</b>	<b>38</b>

## 8 Literature

- 1 Mangelsdorf, D. J. *et al.* The nuclear receptor superfamily: the second decade. *Cell* **83**, 835-839, doi:10.1016/0092-8674(95)90199-x (1995).
- 2 Global, regional, and national incidence, prevalence, and years lived with disability for 310 diseases and injuries, 1990-2015: a systematic analysis for the Global Burden of Disease Study 2015. *Lancet* **388**, 1545-1602, doi:10.1016/s0140-6736(16)31678-6 (2016).
- 3 Libby, P., Lichtman, A. H. & Hansson, G. K. Immune effector mechanisms implicated in atherosclerosis: from mice to humans. *Immunity* **38**, 1092-1104, doi:10.1016/j.immuni.2013.06.009 (2013).
- 4 Falk, E. Pathogenesis of atherosclerosis. *J Am Coll Cardiol* **47**, C7-12, doi:10.1016/j.jacc.2005.09.068 (2006).
- 5 Herrington, W., Lacey, B., Sherliker, P., Armitage, J. & Lewington, S. Epidemiology of Atherosclerosis and the Potential to Reduce the Global Burden of Atherothrombotic Disease. *Circ Res* **118**, 535-546, doi:10.1161/circresaha.115.307611 (2016).
- 6 Borén, J. *et al.* Low-density lipoproteins cause atherosclerotic cardiovascular disease: pathophysiological, genetic, and therapeutic insights: a consensus statement from the European Atherosclerosis Society Consensus Panel. *Eur Heart J* **41**, 2313-2330, doi:10.1093/eurheartj/ehz962 (2020).
- 7 Herrero-Fernandez, B., Gomez-Bris, R., Somovilla-Crespo, B. & Gonzalez-Granado, J. M. Immunobiology of Atherosclerosis: A Complex Net of Interactions. *Int J Mol Sci* **20**, doi:10.3390/ijms20215293 (2019).
- 8 Gutstein, W. H. & Pérez, C. A. Contribution of vasoconstriction to the origin of atherosclerosis: a conceptual study. *Trends Cardiovasc Med* **14**, 257-261, doi:10.1016/j.tcm.2004.07.003 (2004).
- 9 Libby, P. *et al.* Atherosclerosis. *Nat Rev Dis Primers* **5**, 56, doi:10.1038/s41572-019-0106-z (2019).
- 10 Nakashima, Y., Wight, T. N. & Sueishi, K. Early atherosclerosis in humans: role of diffuse intimal thickening and extracellular matrix proteoglycans. *Cardiovasc Res* **79**, 14-23, doi:10.1093/cvr/cvn099 (2008).

- 11 Libby, P., Ridker, P. M. & Hansson, G. K. Progress and challenges in translating the biology of atherosclerosis. *Nature* **473**, 317-325, doi:10.1038/nature10146 (2011).
- 12 Nakashima, Y., Fujii, H., Sumiyoshi, S., Wight, T. N. & Sueishi, K. Early human atherosclerosis: accumulation of lipid and proteoglycans in intimal thickenings followed by macrophage infiltration. *Arterioscler Thromb Vasc Biol* **27**, 1159-1165, doi:10.1161/atvbaha.106.134080 (2007).
- 13 Goldstein, J. L. & Brown, M. S. A century of cholesterol and coronaries: from plaques to genes to statins. *Cell* **161**, 161-172, doi:10.1016/j.cell.2015.01.036 (2015).
- 14 Mundi, S. *et al.* Endothelial permeability, LDL deposition, and cardiovascular risk factors-a review. *Cardiovasc Res* **114**, 35-52, doi:10.1093/cvr/cvx226 (2018).
- 15 Gisterå, A. & Hansson, G. K. The immunology of atherosclerosis. *Nat Rev Nephrol* **13**, 368-380, doi:10.1038/nrneph.2017.51 (2017).
- 16 Nakashima, Y., Raines, E. W., Plump, A. S., Breslow, J. L. & Ross, R. Upregulation of VCAM-1 and ICAM-1 at atherosclerosis-prone sites on the endothelium in the ApoE-deficient mouse. *Arterioscler Thromb Vasc Biol* **18**, 842-851, doi:10.1161/01.atv.18.5.842 (1998).
- 17 Bentzon, J. F., Otsuka, F., Virmani, R. & Falk, E. Mechanisms of plaque formation and rupture. *Circ Res* **114**, 1852-1866, doi:10.1161/circresaha.114.302721 (2014).
- 18 Pasterkamp, G., den Ruijter, H. M. & Libby, P. Temporal shifts in clinical presentation and underlying mechanisms of atherosclerotic disease. *Nat Rev Cardiol* **14**, 21-29, doi:10.1038/nrcardio.2016.166 (2017).
- 19 Owens, A. P., 3rd & Mackman, N. Tissue factor and thrombosis: The clot starts here. *Thromb Haemost* **104**, 432-439, doi:10.1160/th09-11-0771 (2010).
- 20 Otsuka, F. *et al.* The importance of the endothelium in atherothrombosis and coronary stenting. *Nat Rev Cardiol* **9**, 439-453, doi:10.1038/nrcardio.2012.64 (2012).
- 21 Reiner, Z. *et al.* ESC/EAS Guidelines for the management of dyslipidaemias: the Task Force for the management of dyslipidaemias of the European Society of Cardiology (ESC) and the European Atherosclerosis Society (EAS). *Eur Heart J* **32**, 1769-1818, doi:10.1093/eurheartj/ehr158 (2011).

- 22 Zhang, Z. *et al.* Genomic analysis of the nuclear receptor family: new insights into structure, regulation, and evolution from the rat genome. *Genome Res* **14**, 580-590, doi:10.1101/gr.2160004 (2004).
- 23 Chawla, A., Repa, J. J., Evans, R. M. & Mangelsdorf, D. J. Nuclear receptors and lipid physiology: opening the X-files. *Science* **294**, 1866-1870, doi:10.1126/science.294.5548.1866 (2001).
- 24 Weikum, E. R., Liu, X. & Ortlund, E. A. The nuclear receptor superfamily: A structural perspective. *Protein Sci* **27**, 1876-1892, doi:10.1002/pro.3496 (2018).
- 25 Feng, W. *et al.* Hormone-dependent coactivator binding to a hydrophobic cleft on nuclear receptors. *Science* **280**, 1747-1749, doi:10.1126/science.280.5370.1747 (1998).
- 26 Savkur, R. S. & Burris, T. P. The coactivator LXXLL nuclear receptor recognition motif. *J Pept Res* **63**, 207-212, doi:10.1111/j.1399-3011.2004.00126.x (2004).
- 27 Hu, X. & Lazar, M. A. The CoRNR motif controls the recruitment of corepressors by nuclear hormone receptors. *Nature* **402**, 93-96, doi:10.1038/47069 (1999).
- 28 Apfel, R. *et al.* A novel orphan receptor specific for a subset of thyroid hormone-responsive elements and its interaction with the retinoid/thyroid hormone receptor subfamily. *Mol Cell Biol* **14**, 7025-7035, doi:10.1128/mcb.14.10.7025-7035.1994 (1994).
- 29 Willy, P. J. *et al.* LXR, a nuclear receptor that defines a distinct retinoid response pathway. *Genes Dev* **9**, 1033-1045, doi:10.1101/gad.9.9.1033 (1995).
- 30 Repa, J. J. *et al.* Regulation of mouse sterol regulatory element-binding protein-1c gene (SREBP-1c) by oxysterol receptors, LXRalpha and LXRbeta. *Genes Dev* **14**, 2819-2830, doi:10.1101/gad.844900 (2000).
- 31 Glass, C. K. & Rosenfeld, M. G. The coregulator exchange in transcriptional functions of nuclear receptors. *Genes Dev* **14**, 121-141 (2000).
- 32 Duval, C. *et al.* Niemann-Pick C1 like 1 gene expression is down-regulated by LXR activators in the intestine. *Biochem Biophys Res Commun* **340**, 1259-1263, doi:10.1016/j.bbrc.2005.12.137 (2006).
- 33 Graf, G. A. *et al.* ABCG5 and ABCG8 are obligate heterodimers for protein trafficking and biliary cholesterol excretion. *J Biol Chem* **278**, 48275-48282, doi:10.1074/jbc.M310223200 (2003).

- 34 Brunham, L. R. *et al.* Tissue-specific induction of intestinal ABCA1 expression with a liver X receptor agonist raises plasma HDL cholesterol levels. *Circ Res* **99**, 672-674, doi:10.1161/01.RES.0000244014.19589.8e (2006).
- 35 Yu, L. *et al.* Stimulation of cholesterol excretion by the liver X receptor agonist requires ATP-binding cassette transporters G5 and G8. *J Biol Chem* **278**, 15565-15570, doi:10.1074/jbc.M301311200 (2003).
- 36 Peet, D. J. *et al.* Cholesterol and bile acid metabolism are impaired in mice lacking the nuclear oxysterol receptor LXR alpha. *Cell* **93**, 693-704, doi:10.1016/s0092-8674(00)81432-4 (1998).
- 37 Bodzioch, M. *et al.* The gene encoding ATP-binding cassette transporter 1 is mutated in Tangier disease. *Nat Genet* **22**, 347-351, doi:10.1038/11914 (1999).
- 38 Tavoosi, Z. *et al.* Cholesterol Transporters ABCA1 and ABCG1 Gene Expression in Peripheral Blood Mononuclear Cells in Patients with Metabolic Syndrome. *Cholesterol* **2015**, 682904-682904, doi:10.1155/2015/682904 (2015).
- 39 Venkateswaran, A. *et al.* Control of cellular cholesterol efflux by the nuclear oxysterol receptor LXR alpha. *Proc Natl Acad Sci U S A* **97**, 12097-12102, doi:10.1073/pnas.200367697 (2000).
- 40 Ouimet, M., Barrett, T. J. & Fisher, E. A. HDL and Reverse Cholesterol Transport. *Circ Res* **124**, 1505-1518, doi:10.1161/circresaha.119.312617 (2019).
- 41 Kennedy, M. A. *et al.* ABCG1 has a critical role in mediating cholesterol efflux to HDL and preventing cellular lipid accumulation. *Cell Metab* **1**, 121-131, doi:10.1016/j.cmet.2005.01.002 (2005).
- 42 Brown, M. S. & Goldstein, J. L. A receptor-mediated pathway for cholesterol homeostasis. *Science* **232**, 34-47, doi:10.1126/science.3513311 (1986).
- 43 Sun, L. P., Seemann, J., Goldstein, J. L. & Brown, M. S. Sterol-regulated transport of SREBPs from endoplasmic reticulum to Golgi: Insig renders sorting signal in Scap inaccessible to COPII proteins. *Proc Natl Acad Sci U S A* **104**, 6519-6526, doi:10.1073/pnas.0700907104 (2007).
- 44 Brown, M. S. & Goldstein, J. L. The SREBP pathway: regulation of cholesterol metabolism by proteolysis of a membrane-bound transcription factor. *Cell* **89**, 331-340, doi:10.1016/s0092-8674(00)80213-5 (1997).
- 45 Zelcer, N., Hong, C., Boyadjian, R. & Tontonoz, P. LXR regulates cholesterol uptake through Idol-dependent ubiquitination of the LDL receptor. *Science* **325**, 100-104, doi:10.1126/science.1168974 (2009).



- 46 Ishimoto, K. *et al.* Identification of human low-density lipoprotein receptor as a novel target gene regulated by liver X receptor alpha. *FEBS Lett* **580**, 4929-4933, doi:10.1016/j.febslet.2006.08.010 (2006).
- 47 Schultz, J. R. *et al.* Role of LXRs in control of lipogenesis. *Genes Dev* **14**, 2831-2838, doi:10.1101/gad.850400 (2000).
- 48 Joseph, S. B. *et al.* Direct and indirect mechanisms for regulation of fatty acid synthase gene expression by liver X receptors. *J Biol Chem* **277**, 11019-11025, doi:10.1074/jbc.M111041200 (2002).
- 49 Chu, K., Miyazaki, M., Man, W. C. & Ntambi, J. M. Stearoyl-coenzyme A desaturase 1 deficiency protects against hypertriglyceridemia and increases plasma high-density lipoprotein cholesterol induced by liver X receptor activation. *Mol Cell Biol* **26**, 6786-6798, doi:10.1128/mcb.00077-06 (2006).
- 50 Albers, M. *et al.* A novel principle for partial agonism of liver X receptor ligands. Competitive recruitment of activators and repressors. *J Biol Chem* **281**, 4920-4930, doi:10.1074/jbc.M510101200 (2006).
- 51 Dai, S. Y. *et al.* Prediction of the tissue-specificity of selective estrogen receptor modulators by using a single biochemical method. *Proc Natl Acad Sci U S A* **105**, 7171-7176, doi:10.1073/pnas.0710802105 (2008).
- 52 Bischoff, E. D. *et al.* Non-redundant roles for LXRalpha and LXRbeta in atherosclerosis susceptibility in low density lipoprotein receptor knockout mice. *J Lipid Res* **51**, 900-906, doi:10.1194/jlr.M900096 (2010).
- 53 Repa, J. J. & Mangelsdorf, D. J. The role of orphan nuclear receptors in the regulation of cholesterol homeostasis. *Annu Rev Cell Dev Biol* **16**, 459-481, doi:10.1146/annurev.cellbio.16.1.459 (2000).
- 54 Komati, R. *et al.* Ligands of Therapeutic Utility for the Liver X Receptors. *Molecules* **22**, doi:10.3390/molecules22010088 (2017).
- 55 Leonarduzzi, G., Sottero, B. & Poli, G. Oxidized products of cholesterol: dietary and metabolic origin, and proatherosclerotic effects (review). *J Nutr Biochem* **13**, 700-710, doi:10.1016/s0955-2863(02)00222-x (2002).
- 56 Janowski, B. A., Willy, P. J., Devi, T. R., Falck, J. R. & Mangelsdorf, D. J. An oxysterol signalling pathway mediated by the nuclear receptor LXR alpha. *Nature* **383**, 728-731, doi:10.1038/383728a0 (1996).

- 57 Lehmann, J. M. *et al.* Activation of the nuclear receptor LXR by oxysterols defines a new hormone response pathway. *J Biol Chem* **272**, 3137-3140, doi:10.1074/jbc.272.6.3137 (1997).
- 58 Collins, J. L. *et al.* Identification of a nonsteroidal liver X receptor agonist through parallel array synthesis of tertiary amines. *J Med Chem* **45**, 1963-1966, doi:10.1021/jm0255116 (2002).
- 59 Dias, D. A., Urban, S. & Roessner, U. A historical overview of natural products in drug discovery. *Metabolites* **2**, 303-336, doi:10.3390/metabo2020303 (2012).
- 60 Cragg, G. M. & Newman, D. J. Natural products: a continuing source of novel drug leads. *Biochim Biophys Acta* **1830**, 3670-3695, doi:10.1016/j.bbagen.2013.02.008 (2013).
- 61 Farnsworth, N. R., Akerele, O., Bingel, A. S., Soejarto, D. D. & Guo, Z. Medicinal plants in therapy. *Bull World Health Organ* **63**, 965-981 (1985).
- 62 Hamilton, G. R. & Baskett, T. F. In the arms of Morpheus the development of morphine for postoperative pain relief. *Can J Anaesth* **47**, 367-374, doi:10.1007/bf03020955 (2000).
- 63 Koehn, F. E. & Carter, G. T. The evolving role of natural products in drug discovery. *Nat Rev Drug Discov* **4**, 206-220, doi:10.1038/nrd1657 (2005).
- 64 Zhou, X., Zhu, H., Liu, L., Lin, J. & Tang, K. A review: recent advances and future prospects of taxol-producing endophytic fungi. *Appl Microbiol Biotechnol* **86**, 1707-1717, doi:10.1007/s00253-010-2546-y (2010).
- 65 Feher, M. & Schmidt, J. M. Property distributions: differences between drugs, natural products, and molecules from combinatorial chemistry. *J Chem Inf Comput Sci* **43**, 218-227, doi:10.1021/ci0200467 (2003).
- 66 Manners, G. D. Citrus limonoids: analysis, bioactivity, and biomedical prospects. *J Agric Food Chem* **55**, 8285-8294, doi:10.1021/jf071797h (2007).
- 67 Tan, Q. G. & Luo, X. D. Meliaceae limonoids: chemistry and biological activities. *Chem Rev* **111**, 7437-7522, doi:10.1021/cr9004023 (2011).
- 68 Roy, A. & Saraf, S. Limonoids: overview of significant bioactive triterpenes distributed in plants kingdom. *Biol Pharm Bull* **29**, 191-201, doi:10.1248/bpb.29.191 (2006).
- 69 Liang, G. *et al.* Chemistry of the Burseraceae. XI. X-Ray-Diffraction Studies on Some Tirucall-7-ene Triterpenes From *Aucoumea klaineana*

- (Burseraceae). *Australian Journal of Chemistry* **42**, 1169-1175, doi:<https://doi.org/10.1071/CH9891169> (1989).
- 70 Lien, T. P., Kamperdick, C., Schmidt, J., Adam, G. & Van Sung, T. Apotirucallane triterpenoids from *Luvunga sarmentosa* (Rutaceae). *Phytochemistry* **60**, 747-754, doi:10.1016/s0031-9422(02)00156-5 (2002).
- 71 Hernandez, V. *et al.* New Tirucallane-Type Triterpenoids from *Guarea guidonia*. *Planta Med* **84**, 716-720, doi:10.1055/s-0044-100524 (2018).
- 72 Kumar, V., Niyaz, N. M. M., Wickramaratne, D. B. M. & Balasubramaniam, S. Tirucallane derivatives from *Paramignya monophylla* fruits. *Phytochemistry* **30**, 1231-1233, doi:[https://doi.org/10.1016/S0031-9422\(00\)95207-5](https://doi.org/10.1016/S0031-9422(00)95207-5) (1991).
- 73 Passos, M. S. *et al.* Limonoids from the genus *Trichilia* and biological activities: review. *Phytochemistry Reviews* **20**, 1055-1086, doi:10.1007/s11101-020-09737-x (2021).
- 74 Pagna, J. I. M. *et al.* Antibacterial activity of some chemical constituents from *Trichilia prieuriana* (Meliaceae). *Zeitschrift für Naturforschung B* **76**, 439-446, doi:doi:10.1515/znb-2021-0057 (2021).
- 75 Graham, F. L., Smiley, J., Russell, W. C. & Nairn, R. Characteristics of a human cell line transformed by DNA from human adenovirus type 5. *J Gen Virol* **36**, 59-74, doi:10.1099/0022-1317-36-1-59 (1977).
- 76 Tsuchiya, S. *et al.* Establishment and characterization of a human acute monocytic leukemia cell line (THP-1). *Int J Cancer* **26**, 171-176, doi:10.1002/ijc.2910260208 (1980).
- 77 Aden, D. P., Fogel, A., Plotkin, S., Damjanov, I. & Knowles, B. B. Controlled synthesis of HBsAg in a differentiated human liver carcinoma-derived cell line. *Nature* **282**, 615-616, doi:10.1038/282615a0 (1979).
- 78 Giger, E. V. *et al.* Gene delivery with bisphosphonate-stabilized calcium phosphate nanoparticles. *J Control Release* **150**, 87-93, doi:10.1016/j.jconrel.2010.11.012 (2011).
- 79 Jordan, M., Schallhorn, A. & Wurm, F. M. Transfecting mammalian cells: optimization of critical parameters affecting calcium-phosphate precipitate formation. *Nucleic Acids Res* **24**, 596-601, doi:10.1093/nar/24.4.596 (1996).
- 80 Azad, T., Tashakor, A. & Hosseinkhani, S. Split-luciferase complementary assay: applications, recent developments, and future perspectives. *Anal Bioanal Chem* **406**, 5541-5560, doi:10.1007/s00216-014-7980-8 (2014).

- 81 Paguio, A., Stecha, P., Wood, K. V. & Fan, F. Improved dual-luciferase reporter assays for nuclear receptors. *Curr Chem Genomics* **4**, 43-49, doi:10.2174/1875397301004010043 (2010).
- 82 Burnette, W. N. "Western blotting": electrophoretic transfer of proteins from sodium dodecyl sulfate--polyacrylamide gels to unmodified nitrocellulose and radiographic detection with antibody and radioiodinated protein A. *Anal Biochem* **112**, 195-203, doi:10.1016/0003-2697(81)90281-5 (1981).
- 83 Goldring, J. P. D. Measuring Protein Concentration with Absorbance, Lowry, Bradford Coomassie Blue, or the Smith Bicinchoninic Acid Assay Before Electrophoresis. *Methods Mol Biol* **1855**, 31-39, doi:10.1007/978-1-4939-8793-1\_3 (2019).
- 84 Sawamura, T. New Idol for cholesterol reduction? *Clin Chem* **55**, 2082-2084, doi:10.1373/clinchem.2009.134023 (2009).
- 85 Rosenson, R. S., Hegele, R. A., Fazio, S. & Cannon, C. P. The Evolving Future of PCSK9 Inhibitors. *J Am Coll Cardiol* **72**, 314-329, doi:10.1016/j.jacc.2018.04.054 (2018).

## 9 Acknowledgements

An dieser Stelle möchte ich mich bei all denjenigen bedanken, die mich während der Anfertigung dieser Masterarbeit unterstützt und motiviert haben.

Zuerst gilt mein Dank Frau Professor Verena Dirsch, die meine Masterarbeit betreut und es mir somit ermöglicht hat, diese in der Molecular Target Group zu schreiben.

Ein großes Danke an alle Mitarbeiter, die mir tagtäglich mit Rat und Tat zur Seite standen und für eine lustige und entspannte Arbeitsatmosphäre sorgten.

Ein besonderer Dank gilt meiner Betreuerin Mirta Resetar MSc. für ihr Vertrauen in mich. Durch ihre herausragende Expertise konnte ich in kurzer Zeit sehr viel lernen. Ich möchte mich aber auch für die hilfreichen Anregungen und die konstruktive Kritik bei der praktischen Arbeit bedanken.

Von Herzen möchte ich meinem Vater und meiner Mutter für die finanzielle Unterstützung und den ständigen Support danken.

Zum Schluss möchte ich noch meiner Oma, die immer an mich geglaubt hat, Dankeschön sagen.